DOTTORATO DI RICERCA IN

BIOMEDICINA TRASLAZIONALE

(XXXV Ciclo)

Coordinatore

Prof. Carlo Vancheri

Dottorando

Dott. Giuseppe Carota

Neuroprotective role of α-Lipoic Acid in intracerebral hemorrhage-like iron overload model.

Relatori

Prof. Riccardo Polosa

Prof. Giovanni Li Volti

Co-Relatore

Prof. Daniele Tibullo

Index

1. Introduction

1.1 Intracerebral Hemorrhage

Intracerebral hemorrhage (ICH) represents a leading cause of morbidity and mortality in the world, and even in case of patient survival, it is frequently associated with severe long-term disability [1]. ICH is the most common hemorrhagic stroke subtype, with an estimated annual incidence rate of 23.15 per 100,000 worldwide, with higher incidence in males [2]. Spontaneous and non-traumatic ICH can be due to an underlying lesion, although the majority of cases in the adult population are attributable to hypertension, which represents the most common systemic risk factor, present in up to 70% of ICH patients [3]. In addition to symptomatic ICH, occurring of silent microbleeds in healthy adults could lead to asymptomatic conditions of ICH, with higher rate in older people; however, the long-term impact of this kind of micro-hemorrhages is still not well defined [4]. ICH is basically due to a parenchymal arteriole rupture in the brain; beyond hemorrhagic transformation of an ischemic stroke, several other processes could lead to ICH, including tumors, cerebral venous thrombosis, ruptured saccular aneurysms, vascular inflammations and malformations [5]. The blood released after vessel rupture leads to immediate primary brain injury. Furthermore, the extravasated blood within the skull and mechanical compression of local structures affect the intracranial pressure (ICP), causing a higher level of damage in the brain [1, 6]. Despite a high incidence related both to an aging population and the use of common medications, such as anticoagulation and antiplatelet drugs, there is still a limited number of appropriate therapies to face ICH consequences [7, 8].

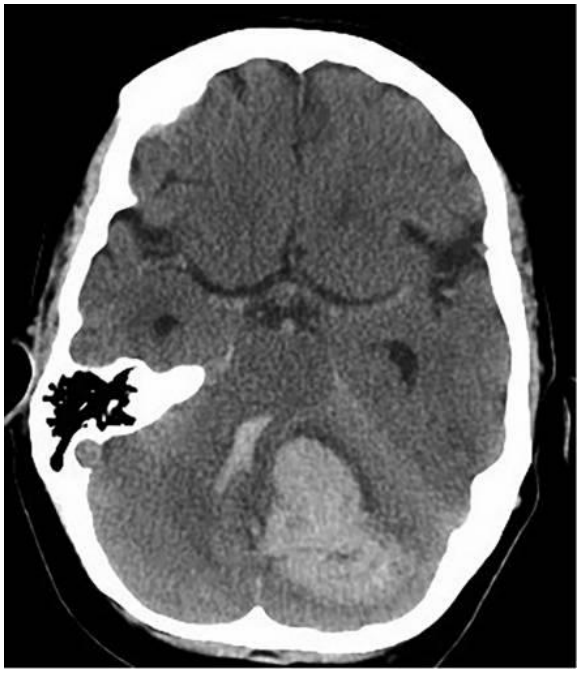

Figure 1. Axial computerized tomography (CT) scan showing spontaneous cerebellar intracerebral hemorrhage with intraventricular extension causing compression of the 4th ventricle and brainstem. (Wilkinson et al. 2019, Neuropharmacology)

The aim of ICH medical management is to treat and control the ICP, the systemic hypertension and to prevent a possible hematoma expansion, especially within 24 hours after stroke [9]. The common approaches used to control primary brain injury involve both surgical and minimally invasive measures, in order to correct the coagulopathy and remove the presence of clot [10]. However, clinical trials have not shown ameliorated conditions after surgical evacuation, probably due to the imbalance between surgery adverse effect and actual evacuation benefits [11, 12]. The physiologic response to the primarily edema and to the toxic effects mediated by clot components (hemoglobin/iron), lead to secondary brain injury: strategies to prevent this condition focus not only on clot removal, but also on pharmacological approaches [13].

1.2 Iron Homeostasis, Toxicity and Overload

Hemoglobin and iron release from hematoma is considered the major contributor to ICH-induced brain injury [14]. A number of pathological brain conditions such as hemorrhage, ischemia, edema and mechanical injury can lead to free heme deposition: in case of ICH, it has been reported that iron liberation into the brain tissue typically begins 24h after hemorrhage, and its deposition and accumulation into perihematomal tissue occurs within few days after ICH [15-17]. As a consequence of red blood cell lysis following ICH, hemoglobin is released into the extracellular space [18]. Hemoglobin contains a globin and four heme groups, and each of them consists of a porphyrin ring with ferrous iron in the center of the molecule. In case of release, the iron oxidizes from ferrous (Fe^{2+}) to ferric (Fe^{3+}). This procedure is the cause of hemoglobin destabilization: it triggers a cascade of inflammatory reactions leading to blood–brain barrier (BBB) disruption, edema occurring, neuronal cell death and secondary brain damage development after ICH [19]. The intracellular amount of iron in neurons and glia originates from cytoplasmic hemoproteins and mitochondrial cytochromes, while the extracellular iron comes from suffering cells and from extravasation of hemoglobin from erythrocytes [20, 21]. The presence of free hemoglobin and iron in brain tissue is suggested to exacerbate oxidative stress and inflammation: because of its potential toxicity, iron content needs to be tightly regulated in the brain [8]. Brain iron homeostasis involves regulation of iron movement between blood, brain and the different iron pools. The iron movement through cell membranes requires specific transport systems: transferrin is able to scavenge and bind free iron (Fe^{3+}) in the extracellular space, and to move it inside cells by endocytosis. In intracellular space Fe^{3+} is reduced to Fe^{2+} and released from endosome into the cytoplasm by Divalent Metal Transporter 1 (DMT1), a protein able to transport a number of divalent and trivalent ions, including iron, zinc, cobalt, copper [22-24]. The cytosolic iron is considered part

of a labile pool, in fact it is both contained in lysosomes and bound by ferritin, able to sequester Fe^{2+} ions in ferroxidase centres. Through these subunits, ferritin is capable to consume all reagents of the radical Fenton reactions, thereby inhibiting iron-mediated oxidative stress [25]. In those conditions in which ferritin level become saturated, iron can be moved out from cells into the cerebral interstitial fluid by Ferroportin 1 (FPN1). In conjunction with this shift, the free Fe^{2+} ions are oxidized to Fe^{3+} by the multicopper ferroxidase ceruloplasmin, allowing transferrin to an easily bound once in the extracellular space [26, 27]. The amount of hemoglobin released into the extracellular space following ICH, may overwhelm the iron homeostatic system. The occurred iron overload due to saturation of these mechanisms, can result in presence of toxic form of iron (Fe^{2+}) involved in harmful reactions such as free radical production, i.e., the above-mentioned Fenton reaction [28, 29].

$$Fe^{2+} + H_2O_2 \rightarrow Fe^{3+} + OH\cdot + OH^-$$

In this reaction, ferrous iron reacts with hydrogen peroxide to form radical oxygen species. The resulting ferric iron can be reduced back to Fe^{2+}, which leads to the restart of the radical reaction cycle. Different cellular antioxidants such as Glutathione (GSH) and Superoxide Dismutase (SOD) work to limit this damage, but their efficacy is not sufficient to combat the amount of oxidative stress occurring after ICH [30, 31]. The radical-induced injuries to DNA, proteins and lipids result in the death of neurons, glia and endothelial cells. The damage occurred to the neurovascular system leads to blood-brain barrier disruption, with subsequent edema development [32]. It has been reported that ICH-mediated iron overload is linked to different types of cell death, such as necrosis, apoptosis, autophagy and ferroptosis [33]. In particular, apoptosis of neurons and astrocytes due to iron release is related to DNA fragmentation, caspase activation and mitochondrial membrane alteration [34-36], while

ferroptosis, an iron-dependent form of cell death, is related to ROS accumulation and cell damage in the way of lipid peroxidation, due to the disruption of dynamic balance between antioxidant system and oxidant agents [37, 38]. The iron-mediated cell death promotion is also conducted by microglia activation: together with neutrophils, microglia release toxic substances (thrombin, ROS, metalloproteinases), leading to neuroinflammation and oxidative stress, which are responsible for the increase of the level of pro-inflammatory cytokines, such as tumor necrosis factor-α (TNF-α) and interleukin-6 (IL-6) [39, 40]. In this context, it is highly confirmed that brain accumulation of iron after ICH represents one of the main responsible for neurodegeneration, brain atrophy and long-term neurological deficits occurred after ICH [41].

1.3 Microglia

Microglia are unique myeloid cells residing in the parenchyma of the healthy central nervous system (CNS). These cells arise from erythro-myeloid precursors and become part of the brain innate immune system early during development. Although similar aspects in common with monocyte-derived macrophages, microglia are characterized by specific functional properties which make them unique among other populations of myeloid cells present in the brain, such as perivascular macrophages, meningeal macrophages, and choroid plexus macrophages [42, 43]. Unlike monocytes, which are constantly renewed from bone marrow hematopoietic stem cells, microglial cells in healthy brain persist due to self-renewal, without turnover from circulating blood precursors [44]. The main function of microglia is to constantly monitor the CNS microenvironment: these cells are able to detect extracellular changes and to react by becoming activated in response to different stimuli. This activity is essential in brain homeostasis regulation during development and in the adult brain, both in physiological and pathological conditions [45]. Like other macrophages, microglia own two main functions, conceptually defined as the ability to kill/fight or to heal/fix. Within this classification view, there are two different microglial phenotypes, M1 and M2, related to killing/fighting and healing/fixing activity respectively, which are relevant in immune response ongoing [46]. This classification can be also condensed into two opposing pathways for arginine metabolism: the preference of microglia to metabolize arginine via nitric oxide synthase (NOS) to NO and citrulline or via arginase (ARG) to ornithine and urea defines them as M1 (NOS) or M2 (ARG) microglial cells [47, 48]. The M1/M2 paradigm is a simplified model to decipher the two faces of the inflammatory response, that justifies microglia activation and polarization, which represent a time and tissue dependent system that implicates intrinsic, extrinsic, and tissue environment stimuli including cytokines, growth factors, fatty acids and prostaglandins [49].

Basing on a simple dichotomic view, microglia is classified as M1 in case of pro-inflammatory phenotype, and M2 in case of anti-inflammatory phenotype [50].

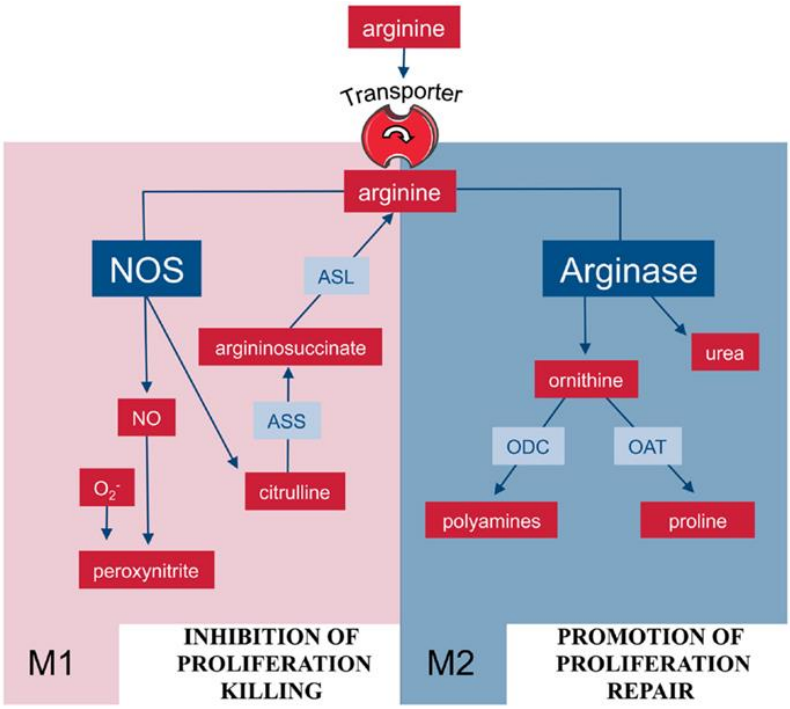

Figure 2. Arginine metabolism via NOS or Arginase is at the center of the M1/M2 polarization of macrophages. (Rath et al. 2014, Frontiers in Immunology)

Microglial activation in response to pro- and anti- inflammatory stimuli is characterized both as classical M1 and alternative M2: M1 activation is pro-inflammatory and neurotoxic and is primarily induced through the activation of toll-like receptor (TLR) and interferon gamma (IFN-γ) signaling pathway [51]. M1 microglia are able to secrete pro-inflammatory cytokines and chemokines including TNF-α and different members of the interleukin family, such as interleukin-6 (IL-6), interleukin 1-beta (IL-1β), interleukin-12 (IL-12) [52]. When activated as M1, microglia drive arginine metabolism via NOS, leading to an overexpression of inducible nitric oxide synthase (iNOS, or NOS2) and a subsequent accumulation of NO, which is known

to increase the toxic effects of glutamate and the N-methyl-D-aspartate (NMDA) receptor-mediated neurotoxicity [53, 54]. On the other hand, microglia in M2 state release anti-inflammatory cytokines including interleukin-4 (IL-4), interleukin-10 (IL-10), interleukin-13 (IL-13) and transforming growth factor-beta (TGF-β). Furthermore, the arginine metabolism via ARG avoids the accumulation of NO, and ornithine produced from arginine catabolism is transformed by ornithine decarboxylase (ODC) to polyamines (putrescine, spermidine, and spermine) that control cell growth and are important for tissue repair [55, 56]. M2 microglia can also secrete important neurotrophic factors involved in inflammation solving and synaptic plasticity promotion, such as nerve growth factor (NGF) and brain-derived neurotrophic factor (BDNF) [57]. Hence, the dichotomic view of M1/M2 condition oversimplifies a complex process for microglial activity: transcriptome studies have shown that microglia activation is variable and context-dependent, meaning that M1 and M2 represent a spectrum of activation patterns rather than separate cell phenotypes, thus the M1/M2 paradigm is inadequate to accurately describe the dynamic microglia activation system *in vivo* [58-60]. Microglia can transit from one phenotype to another according to different environments in the CNS, exerting the known protective role by switching their phenotype. Indeed, microglia adopt a homeostatic (M0) state under normal conditions in the CNS, and their transcriptome profile reflects their immunosurveillance activities in this state [61]. As key innate immune cells, microglia act as guardians of the brain and are recognized to be the first non-neuronal cells to respond to various acute brain injuries, including ICH [62]. Microglia become activated immediately after ICH, make morphological changes from a highly ramified phenotype to a rod, spherical, and finally an amoeba shape [63]. In the time course, microglia activation begins within 1–4 h, peaks in 1–3 days, declines at day 7, and returns to physiological level in 3–4 weeks after ICH [64, 65]. Since M1/M2 proportion is continually changing, both M1 and

M2 phenotypes are present in the perihematomal area after ICH. The M1 state is preponderant for 7 days after ICH, while the polarization changes in M2 state within 10-14 days [66].

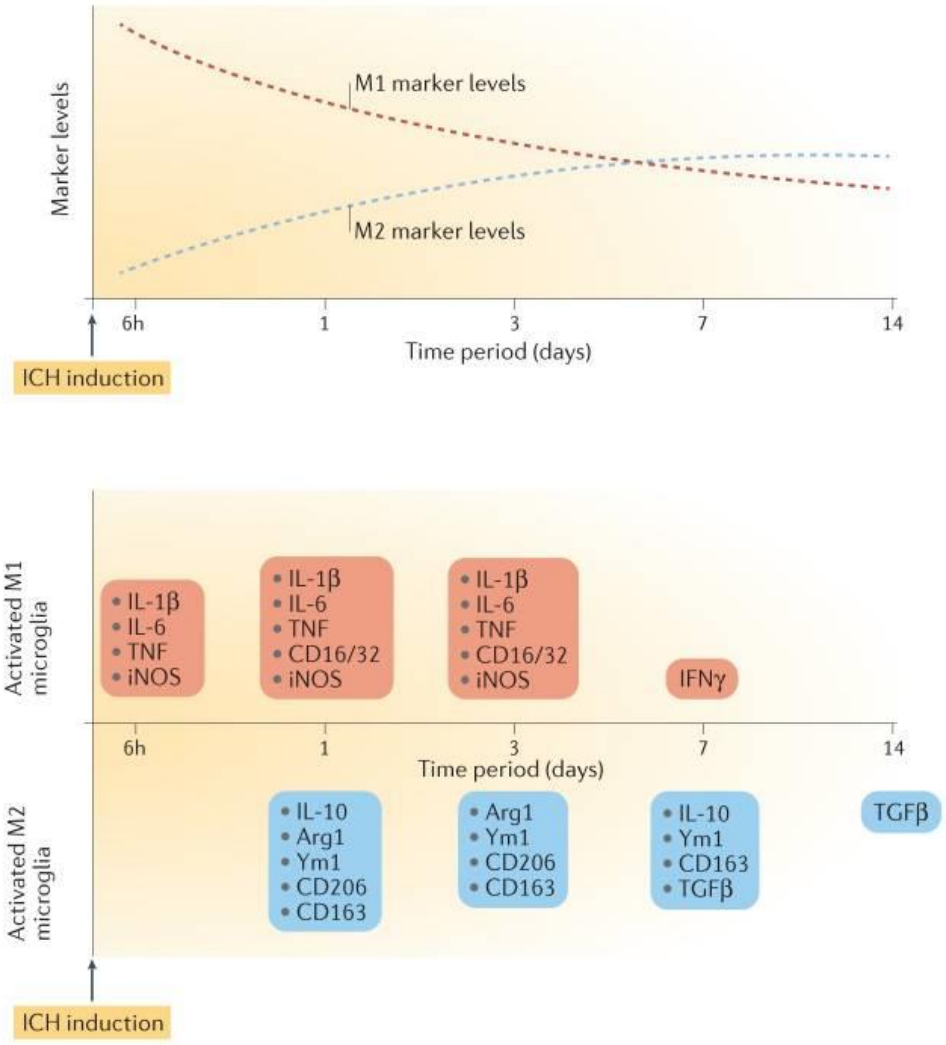

Figure 3. Dynamic changes in microglial marker levels and profiles over time after intracerebral hemorrhage. (Lan et al. 2017, Nature Reviews Neurology)

The stress condition due to inflammatory cytokines diffusion after ICH leads to neurons and neuroglia death, and promote the polarization of surrounding microglia towards the M1 phenotype, which forms a vicious circle [67]. M1 microglia increase expression of peroxidases, NOS2, and reduced form of nicotinamide-adenine dinucleotide phosphate (NADPH) oxidase, that lead to excessive free radicals' production and consequent cell damage [68]. Moreover, M1 microglia contribute to the activation of matrix metalloproteinases (MMPs), including MMP2 and MMP9, which markedly affect the BBB integrity and cause severe vasogenic brain edema by degrading extracellular matrix constituents and attacking endothelial claudin-family tight junction proteins [69]. M2 microglia are perceived to be an essential participant in long-term recovery after ICH. In contrast with M1 phenotypic markers, increased expression of M2 phenotypic markers emerge much later and last longer. M2 microglia primarily facilitate tissue regeneration by phagocytizing the hematoma and cells debris and by removing harmful substances from the affected space. With the increase of the number of M2 microglia, the volume of the hematoma is eliminated promptly in 7–21 days after ICH [70, 71]. In order to promote tissue regeneration and remodeling, M2 microglia express several growth and trophic factors, including BDNF, glial cell line-derived neurotrophic factor (GDNF), neurotrophin 3 (NT-3) and insulin-like growth factors-1 (IGF-1) [72, 73]. The M2 cell's ability to resist inflammation and to reduce hematomas, contributes to the neuro-angiogenesis and matrix deposition, and allows brain to regain structure and function. However, due to the contemporaneous presence of M1 microglia, only a slight part of neuron population can survive inflammation in the acute phase. Therefore, the management of microglial phenotypic switch could be considered as a promising strategy to treat ICH consequences [74]. One of the most important markers of neuroinflammation ICH-related, is represented by the increased acquisition of extracellular iron and subsequent intracellular iron sequestration, which is

associated with neuronal degeneration and microglial secretion of inflammatory cytokines [75, 76]. It has been reported that microglia iron transport pathways are differentially active in response to pro- and anti- inflammatory stimuli: pro-inflammatory mediators increase the uptake of iron exploiting the ferritin storage pool, thus upregulating DMT1 and ferritin as well. The uptake of free iron by microglia reduces the potential damage in neural environment due to ROS production [77]. The over-expression of DMT1 during pro-inflammatory state, as pH dependent transporter, is due to an increased glycolytic activity in microglial M1 cells, which supports changes in microenvironment through extracellular acidification, leading to an increased free iron uptake [78].

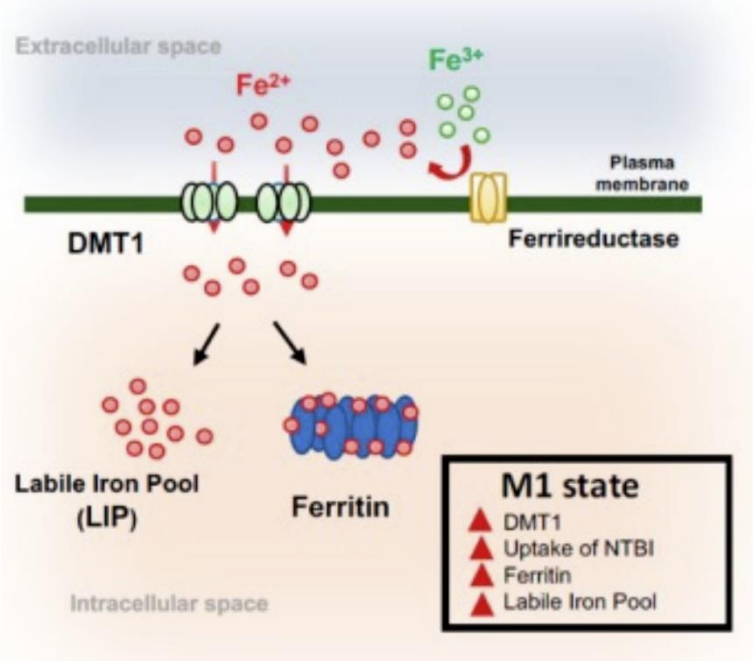

Figure 4. Iron trafficking and microglial cell polarization. Pro-inflammatory stimuli upregulate the expression of DMT-1 and the uptake of non-Transferrin-bound iron (NTBI). These effects are associated with increased labile iron and an expanded pool of ferritin. These changes reflect M1 polarization. (Nnah et al. 2018, Pharmaceuticals)

Inflammatory mediators reduce both oxidative respiration and the levels of intracellular heme by induction of heme oxygenase-1 (HO-1), the responsible enzyme for degradation of heme into carbon monoxide, Fe^{2+} and biliverdin [79]. These changes are associated with increased levels of intracellular iron, suggesting that microglia are able to sequester both intracellular iron released by heme catabolism and extracellular iron moved by DMT1. On the other hand, an anti-inflammatory condition increases the expression of transferrin receptor, therefore promoting iron uptake. Furthermore, M2 microglia could be able to support the regeneration of neurons and the activity of oligodendrocytes through the release of ferritin stores, promoting a shift of iron transport [80].

1.4 α-Lipoic Acid

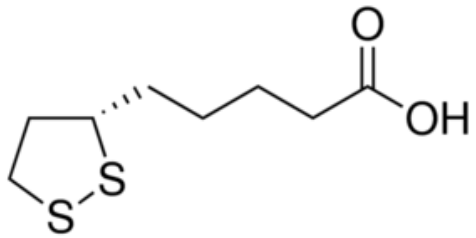

Figure 5. α-Lipoic Acid (1,2-dithiolane-3-pentanoic acid) chemical structure.

α-Lipoic Acid (1,2-dithiolane-3-pentanoic acid; thioctic acid; Alpha-Lipoic Acid) (ALA) is an active organosulfur compound, naturally synthesized by plants and animals [81]. Both the oxidized (disulfide) and reduced (di-thiol: dihydro-lipoic acid, DHLA) forms of ALA show antioxidant properties. ALA exists as two different enantiomers: the biologically active (R)-isomer and the (S)-isomer. Commercial ALA is usually a racemic mixture of the R- and S-form [82]. ALA is both water and lipid soluble and is widely distributed in cellular membranes, cytosol, and extracellular spaces. It is absorbed from the diet and is able to cross the BBB and cell monolayer in a pH-dependent manner, without causing any toxicity at therapeutic doses. Cellular transport of ALA occurs probably via several systems, such as the medium-chain fatty acid transporter, an Na^+-dependent vitamin transport system, and an H^+-linked monocarboxylate transporter for intestinal uptake [83]. ALA transport can be inhibited by compounds such as benzoic acid and medium-chain fatty acids, suggesting that the monocarboxylate transporter could be the likely carrier responsible for intestinal absorption of ALA [84]. ALA is a powerful neuroprotective antioxidant, and has proven to be effective in the treatment of several oxidative stress-related diseases, such as diabetes, ischemic reperfusion damage and radiation injury [85-88]. As strong antioxidant, ALA is involved in a

number of cellular processes, including direct radical scavenging, recycling, metal chelation, modulation of transcription factor activity and regeneration of endogenous antioxidants. In this regard, ALA has been reported to ameliorate endothelial function and blood flow, and to accelerate GSH synthesis, which plays a crucial role in regulating the expression of several antioxidant and anti-inflammatory genes [89-91]. The efficacy of ALA as iron chelator has been demonstrated in a combined treatment with ferric ammonium citrate (FAC), simulating an iron overload condition both *in vitro* and *in vivo*. Administration of ALA in mesenchymal stem cells led to a decrease of ROS levels and a restoring of mitochondrial membrane potential and integrity, following the treatment with FAC. Augmented levels of GSH have been associated with the direct antioxidant effect of ALA, leading to enhanced antioxidant defenses for the cells. Consequently, through the increase of intracellular GSH content, ALA prevented the nuclear factor erythroid 2–related factor 2 (NRF2) pathway activation, leading to the reduction of HO-1 expression. The same result has been confirmed in an *in vivo* model of zebrafish, with significant reduction of heme oxygenase 1b (HMOX1b), mitochondrial superoxide dismutase (mtSOD), and FPN1 expression after treatment with ALA in the presence of an iron overload [92]. Following different *in vivo* experiments, Zhao et al. demonstrated the capacity of ALA as iron chelator to prevent the light-induced retinal degeneration in a mouse model of AMD (age-related macular degeneration) through systemic administrations [93]. The role of ALA in microglia context is not fully known, but it has been shown a number of effects of ALA affecting microglia including inhibition of phagocytosis, reorganization of actin, prevention of upregulation of iNOS (and the related control on microglia activation) and inhibition of Akt/glycogen synthase kinase-3ß [94-96]. Abnormally high levels of iron in the brain have been demonstrated in a number of neurodegenerative disorders, such as Alzheimer's disease and Parkinson's disease (PD). The neuroprotective effect of ALA was tested in a PD model induced

by 6-hydroxydopamine (6-OHDA), showing significant reduction of ROS and an improvement of iron metabolism levels, confirming the therapeutic potential of ALA for the treatment of neurodegenerative diseases associated with iron metabolism dysfunction and oxidative stress [97]. Furthermore, due to the increased iron and ROS levels in the body and the related lung fibrosis generation during COVID-19 disease, several studies have been conducted to find any substance capable to reduce and partially control the severity of the infection. Through their iron chelation effect, substances like Deferoxamine were shown to reduce iron availability in the serum and body tissue, preventing lung injury and fibrosis following COVID-19 infection [98]. It has been shown that some important natural products with an amply demonstrated activity as iron chelators and protease inhibitors, such as ALA, are suggested to be a possible therapeutical strategy toward the pathological context related to COVID-19 infection [99].

2. Materials and methods

2.1 Cell culture and treatments

HMC3 human microglial cells were purchased from ATCC Company (Milan, Italy). Cells were cultured in Minimum Essential Medium (MEM) supplemented with 10% fetal bovine serum (FBS), 100 U/mL penicillin, 100 U/mL streptomycin and 1% L-glutamine, and were maintained in a humidified incubator at 37 °C with 95% air/5% CO_2. At 80% confluency, cells were passaged using trypsin-EDTA solution (0.25% trypsin and 0.02% EDTA). The cells were pre-treated with α-Lipoic Acid (ALA) 100 µM for 3h, while the iron overload was obtained by treating with ferric ammonium citrate (FAC, Alfa Aesar- Thermofisher) 400 µM for 24h. In order to better appreciate changing in gene expression, in this set of experiments the exposure to FAC was reduced also to 6h. Concentrations were selected following results obtained by Camiolo et al. [92, 100].

2.2 xCELLigence real-time cell analysis

xCELLigence experiment was performed using the RTCA (Real-Time Cell Analyzer) DP (Dual Plate) instrument according to manufacturers' instructions (Roche Applied Science, Mannheim, Germany; ACEA Biosciences, San Diego, CA, USA). Cells were seeded in E-16 xCELLigence plates at a density of 5×10^3 cells/ml per well. The plates were then incubated at 37 °C, 5% CO_2 for 30 min in order to allow cell settling. After incubation, cells were treated with FAC 400 µM. Real-time changes in electrical impedance were measured and expressed as "cell index", defined as (Rn-Rb)/15, where Rb is the background impedance and Rn is the impedance of the well with cells. The background impedance was measured in E-plate 16 with 100 µL medium (without cells) after 30 min incubation period at room temperature. Cell proliferation was monitored every 20 min for 48 h.

2.3 Apoptosis evaluation

Annexin V and propidium iodide (PI) staining were used to assess apoptosis. The evaluation was performed by flow cytometry. Samples (2×10^5 cells) were washed twice and resuspended in 100 µL of PBS. 1µL of Annexin V-FITC solution and 5µl of dissolved PI (Beckmam Coulter, made in France) were added to cell suspension and mixed gently. Cells were incubated for 15 minutes in the dark. Finally, 400 µl of 1X binding buffer was added and cell preparation was analyzed by flow cytometry (MACSQuant Analyzer 10, Miltenyi Biotec).

2.4 ROS Analysis

Reactive oxygen species (ROS) were detected using 2',7'-dichlorodihydrofluorescein acetate (H2-DCF; Sigma-Aldrich, St. Louis, MO, USA), and fluorescence intensity was measured according to the fluorescence detection conditions of FITC by using a MACSQuant Analyzer (Miltenyi Biotech, North Rhine-Westphalia, Germany).

2.5 GSH content measurement

Intracellular content of reduced glutathione (GSH) was measured using a spectrophotometric assay based on the reaction of thiol groups with 2,2-dithio-bis-nitrobenzoic acid (DTNB) at λ = 412 nm (εM = 13,600 $M^{-1} \cdot cm^{-1}$, where εM is a wavelength-dependent molar absorptivity coefficient). Measurements were performed in triplicate.

2.6 Mitochondrial membrane potential and mitochondrial mass

A membrane potential probe, the 3,3'-diethyloxacarbocyanine iodide (DiOC2(3)), was used to evaluate the mitochondrial membrane potential. Cells were incubated with 10 µM DiOC2(3) (Thermo Fisher Scientific, Milan, Italy) for 30 min at 37 °C, washed twice, resuspended in PBS and analyzed by flow cytometry through the detection of the green fluorescence intensity of DiOC2(3). In order to measure changes in the mitochondrial mass, cells were reacted with 200

nM MitoTracker Red CMXRos probe (Thermo Fisher Scientific, Milan, Italy) for 30 min at 37 °C, according to the manufacturer's instructions. After being washed twice, labelled mitochondria were analyzed by flow cytometry.

2.7 Real-Time PCR for Gene Expression Analysis

RNA was extracted by Trizol® reagent (category no. 15596026, Invitrogen, Carlsbad, CA, USA). The first-strand cDNA was then synthesized with High-Capacity cDNA Reverse Transcription kit (category no. 4368814, Applied Biosystems, Foster City, CA, USA). High cDNA quality was checked, taking into consideration the housekeeping gene Ct values. Quantitative real-time PCR was performed in Step-One Fast Real-Time PCR system, Applied Biosystems, using SYBR Green PCR MasterMix (category no. 4309155, Life Technologies, Monza, Italy). The specific PCR products were detected by the fluorescence of SYBR Green, the double-stranded DNA binding dye. Primers were designed using BLAST® (Basic Local Alignment Search Tool, NBCI, NIH), considering the shortest amplicon proposed (primers' sequences are shown in Tables 1,2), and GAPDH was used as the housekeeping gene. Primers were purchased from Metabion International AG (Planneg, Germany). The relative mRNA expression level was calculated by the threshold cycle (Ct) value of each PCR product and normalized with GAPDH by using a comparative $2^{-\Delta\Delta Ct}$ method.

Gene (Human)	Forward Primer (5′ → 3′)	Reverse Primer (5′ → 3′)
HO-1	GTTGGGGTGGTTTTTGAGCC	TTAGACCAAGGCCACAGTGC
DMT1	CGGAATAGGAAGTGCCATCCA	GGGAGCAAGGAAAAAGAACTACA
FPN1	CTCCCAAACCGCTTCCATAAG	TCTTCTGCGGCTGCTATCG
COX-2	ATACGACTTGCAGTGAGCGT	GGGTGGGAACAGCAAGGATT
IL-6	CCACCGGGAACGAAAGAGAA	GAGAAGGCAACTGGACCGAA
IL-1β	AGCTCGCCAGTGAAATGATG	GTCGGAGATTCGTAGCTGGA
TNF-α	GCAACAAGACCACCACTTCG	GATCAAAGCTGTAGGCCCCA
ATP5B	AGCTCAGCTCTTACTGCGG	GGTGGTAGTCCCTCATCAAACT
CYTB	TCCTCCCGTGAGGCCAAATATCAT	AAAGAATCGTGTGAGGGTGGGACT
NDUFS4	GATTGGCACAGGACCAGACT	GTTGGATAAGGGATCAGCCGT
TFAM	CCAAAAAGACCTCGTTCAGCTT	CTTCAGCTTTTCCTGCGGTG
GAPDH	TTCTTTTGCGTCGCCAGCC	CTTCCCGTTCTCAGCCTTGAC

Table 1. Primers sequences used to assess gene expression in cells (Human).

Gene (Zebrafish)	Forward Primer (5′ → 3′)	Reverse Primer (5′ → 3′)
hmox1b	CTCTCCAGCCCTTCAGTTCG	AAGCGTAAACTCCCATGCCA
sod1	GTGACAACACAAACGGCTGC	GGCATCAGCGGTCACATTAC
ptgs1	ACTTTACCACTGGCACCCAC	ACGATGACCCTCTCAGCAAC
gapdh	CATCTTTGACGCTGGTGCTG	TGGGAGAATGGTCGCGTATC

Table 2. Primers sequences used to assess gene expression in brain lysate (Zebrafish).

2.8 IL-6 levels determination

ELISA kit was used to measure the concentration of IL-6 in medium conditioned by treatments (ThermoFisher Scientific). The assay was performed according to the manufacturer protocols. Absorbance was measured at a wavelength of 450 nm and biomarker concentrations were calculated from a standard curve generated with purified proteins. The detection limits, as specified by the manufacturer, was 0.92 pg/mL. Each measurement was performed in triplicate.

2.9 Immunofluorescence analysis In Vitro

Cells were grown directly on coverslips before immunofluorescence. After washing with PBS, cells were fixed in 4% paraformaldehyde (Sigma-Aldrich, Milan, Italy) for 20 min at room temperature. After fixation, cells were washed three times in PBS for 5 min and blocked in Odyssey Blocking Buffer for 1 h at room temperature. Subsequently, the cells were incubated with primary antibody against Arginase1 (mouse, Cat. sc-271430, Santa Cruz Biotechnology) and NOS2 (mouse, Cat. sc-7271, Santa Cruz Biotechnology), overnight at 4°C. Next day, cells were washed three times in PBS for 5 min and incubated with secondary antibodies: TRITC (anti-mouse, Cat. No. A11003, ThermoFisher Scientific, Oregon, USA), and FITC (anti-mouse, Cat. No. F2012, Sigma-Aldrich, Missouri, USA) for 1 h at room temperature. The antibodies were diluted in Odyssey Blocking Buffer. The slides were mounted with medium containing DAPI (40, 6-diamidino-2-phenylindole, SantaCruz Biotechnology) to visualize nuclei. The fluorescent images were obtained using a Zeiss Axio Imager Z1 Microscope with Apotome 2 system (Zeiss, Milan, Italy).

2.10 Animals

Adult wildtype AB zebrafish (n = 5, for each group) were used for this study. Fishes were tested to be free from Pseudoloma neurophilia, Pseudocapillaria tomentosa, Mycobacterium spp., and Edwardsiella ictalurias determined by twice-yearly sentinel monitoring. Fishes were housed at a density of 5 fishes per tank in mixed-sex groups in 2.5 L tanks on a recirculating system in 28°C water in a room with a 14:10 h light:dark cycle. System water was carbon-filtered municipal tap water, filtered through a 20 µm pleated particulate filter, and exposed to 40 W UV light. Standard feeding protocol was three meals daily of Tetra-Min (Tetra) in the CAPIR (University of Catania) facility. All zebrafish experiments were performed with the approval of the Animal Studies Committee of Ministero della Salute Italy (Approval code: 814/2017-PR, 23 October 2017). Each experimental group (n = 5) was randomly assigned to a different treatment condition (FAC 400 µM, ALA 100 µM, FAC 400 µM + ALA 100 µM). The chemical agents tested were introduced into a static 2 L tank filled with system water obtained from the main recirculating system. A behavioral control group of untreated fish housed under the same conditions as the experimental groups was tested in parallel. The different groups were observed for 120h. The treatment procedure was scheduled as follow (Figure 6). In opposite to what shown in *in vitro* model, the experiment was performed pre-treating with FAC 400 µM and then treating with ALA 100 µM.

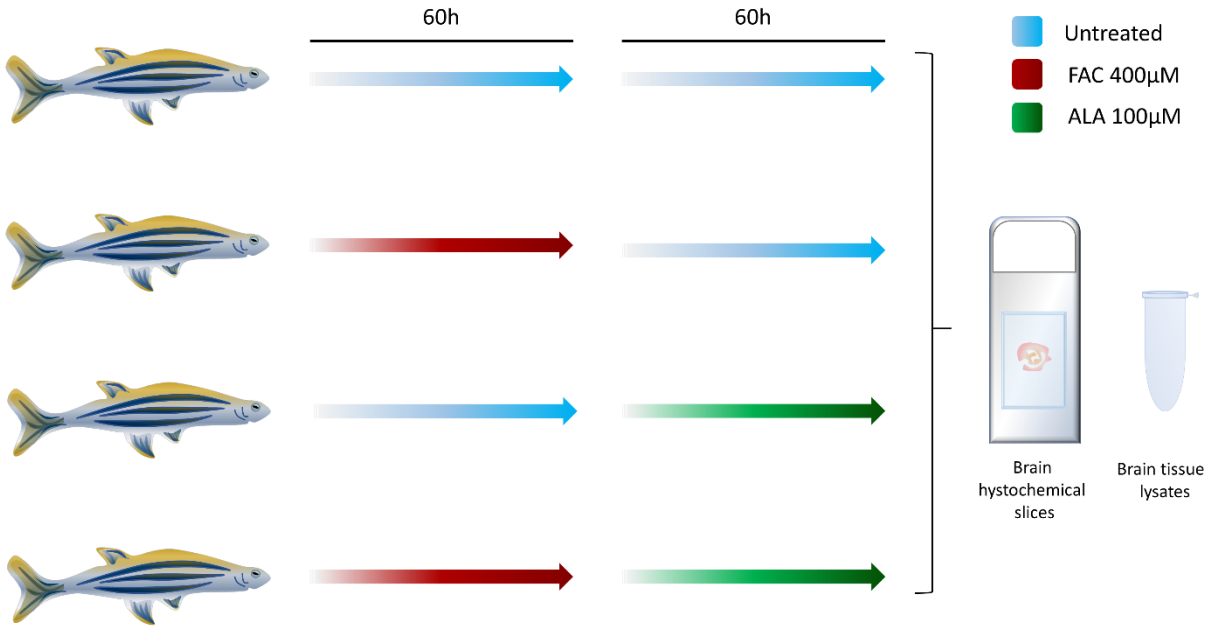

Figure 6. Schematic explanation of *in vivo* treatment procedure.

2.11 Morphological Analysis

Zebrafish brain tissues were collected and fixed in 10% buffered-formaldehyde; after an overnight wash, specimens were dehydrated in graded ethanol and paraffin-embedded, preserving their anatomical orientation. Three to four micrometer thick sections were obtained according to routine procedures, mounted on sialane-coated slides and air-dried. Slides were dewaxed in xylene, hydrated using graded ethanol, and stained for histological studies.

2.12 Perls staining

Perls staining (Bio-Optica, Milan, Italy) was performed according to the manufacturer's instructions. Briefly, tissue sections were passaged in distilled water and stained with Perls staining for 20 min. Sections were then rinsed in distilled water, dehydrated in ascending alcohols, cleared in xylene, and finally mounted for microscopic analysis.

2.13 Immunofluorescence analysis In Vivo

Sections were blocked with a blocking solution (3% H_2O_2 in PBS) for 15 min at room temperature in a humidity chamber. After three washing in PBS for 5 min, sections were incubated for 40 min at room temperature in a humidity chamber with the following primary antibody, diluted in 0.3% Triton X100 in PBS: mouse monoclonal anti-GFAP (BD Biosciences, Cat# 610566, RRID: AB_397916) (1:100). Three washes were performed in 0.3% Triton X100 in PBS for 5 min and sections were incubated with biotinylated panspecific secondary antibody (Horse Anti-Mouse/Rabbit/Goat IgG Antibody (H + L), Cat.No BA-1300-2.2) and diluted in PBS and 1% bovine serum albumin (BSA, Sigma-Aldrich, Cat.No. A2058) for 30 min at room temperature in a humidity chamber. Then VECTASTAIN® Elite ABC-HRP Reagent, Peroxidase, R.T.U. (Vector Laboratories, Milan, Italy, Cat.No PK-7100) was added and sections were incubated for 30 min at room temperature in a humidity chamber, with a 5 min wash in the between. Slides were then washed in 0.1% Triton X-100 in PBS three times at room temperature for 5 min and a solution of 1% DAB and 0.3% H_2O_2 in PBS was added until brown coloration. Then, slides were washed in tap-water for 5 min. Nuclei were counterstained with Mayer's hematoxylin (Bio-Optica, Milan, Italy), dehydrated with increasing concentrations of ethanol (50%, 70%, 95%, 100%) and xylene, and cover-slipped with Entellan (Merck Millipore, Cat.No. 1.079.600.500). Digital images were acquired using the Nexcope NIB600 biological microscope.

2.14 Statistical analysis

Data are shown as means ± standard deviation (SD). For statistical analysis, Prism 8.0.2. software (GraphPad Software, USA) was used. Significant differences between groups were assessed using the one-way ANOVA test. All *in vitro* tests were performed in triplicate, and significance was determined at $p < 0.05$.

3. Results

3.1 FAC affects cell proliferation

In order to confirm the toxicity induced by FAC on cell proliferation, dynamic changes in microglia cell index were monitored for 48h using the xCELLigence system upon exposure to FAC 400 µM. The concentration used was chosen following the results previously obtained by our group [92, 100]. Results show that the presence of FAC starts to affect the proliferation rate of HMC3 microglia cell line after 4h, marking a crescent difference comparing to control along the first day of monitoring. After 24h, the proliferation rate of treated cells was arrested, as shown by the descending curve related to HMC3 cell index (Figure 7).

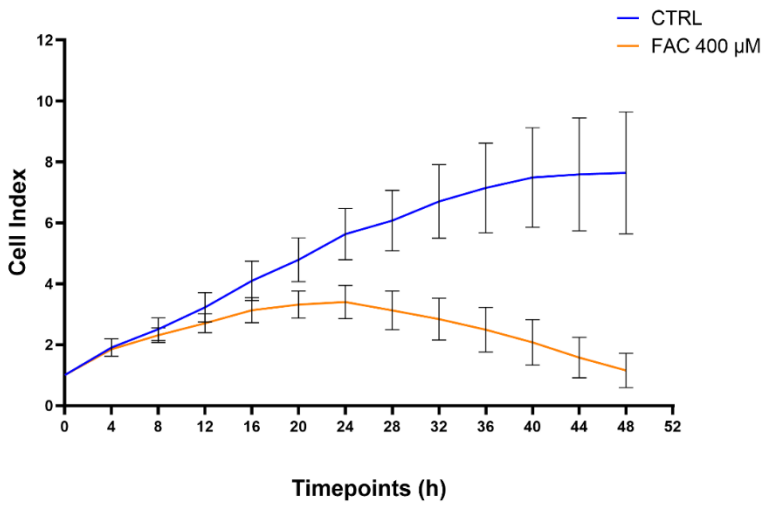

Figure 7. Real-time analysis of cell proliferation in presence of FAC 400 µM (48h).

3.2 ALA reduces apoptosis caused by FAC

The apoptosis rate of HMC3 cells in presence of FAC and ALA was measured by flow cytometry using Annexin V and propidium iodide (PI) staining. Figure 8 shows that iron overload induced by treatment with FAC 400 µM (24h) significantly affected apoptosis rate of HMC3 cells compared to control. In contrast, pre-treatment with ALA 100 µM (3h) [92] was able to prevent the apoptotic condition led by FAC treatment, showing an apoptosis rate similar to untreated cells.

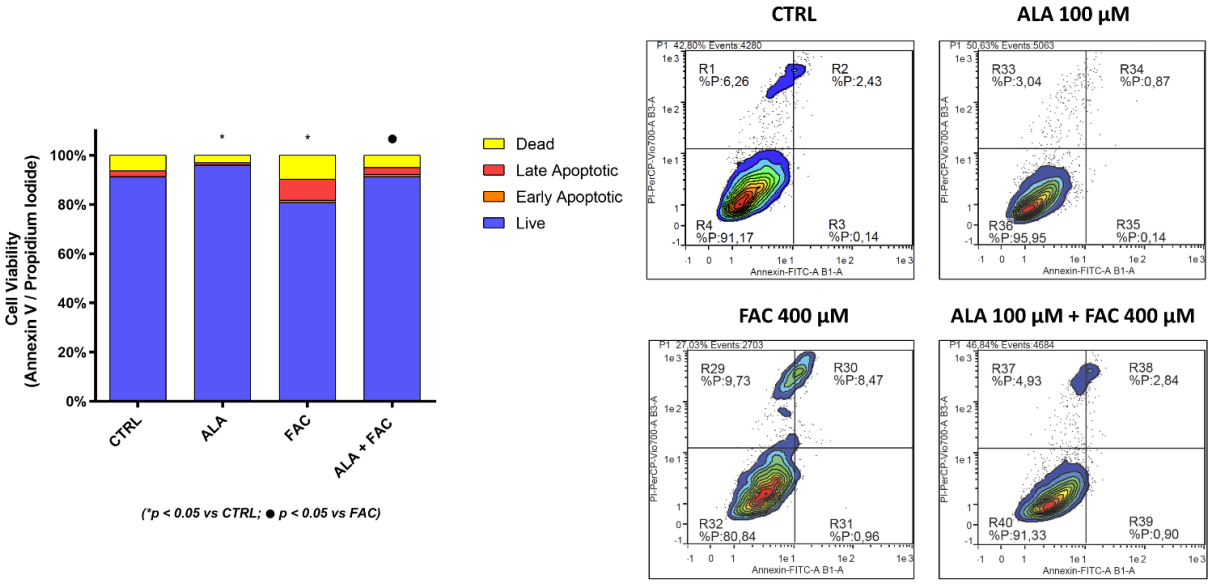

Figure 8. Apoptosis rate analysis by flow cytometry. HMC3 cells were pre-treated with ALA 100 µM (3h), then treated with FAC 400 µM (24h).

3.3 Expression of iron-related markers

In order to observe specific changes in gene expression, HMC3 cells were pre-treated with ALA and then exposed to FAC for 6h. Figure 9A shows that HO-1, the main enzyme involved in heme degradation but also in inflammation and oxidative stress, was upregulated in presence of FAC. Contrarily, the combined presence with ALA reduced HO-1 gene expression to control level. Treatment with FAC led to the significant over expression of DMT1 and FPN1, mainly involved in iron transport (Figure 9B, 9C). Their gene expression followed the same trend, with a decreased level in presence of ALA pre-treatment.

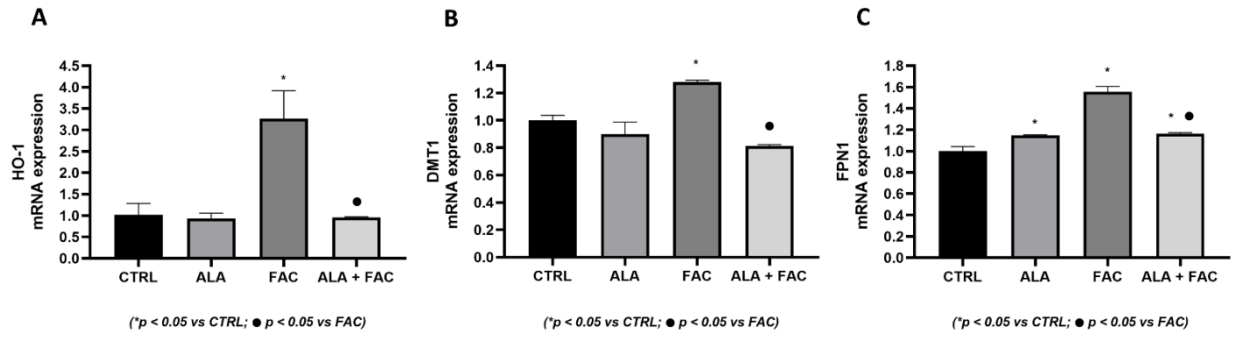

Figure 9. Gene expression of iron-related markers. HMC3 cells were pre-treated with ALA 100 µM (3h), then treated with FAC 400 µM (6h).

3.4 Iron overload affects mitochondrial membrane potential

The mitochondrial membrane potential was assessed by flow cytometry using DiOC2 as probe (Figure 10). The increase of DiOC2 levels is associated to mitochondrial membrane depolarization, related to mitochondrial damage. Iron overload caused a high level of depolarization compared to untreated healthy cells, whereas the combined presence with ALA restored the membrane potential.

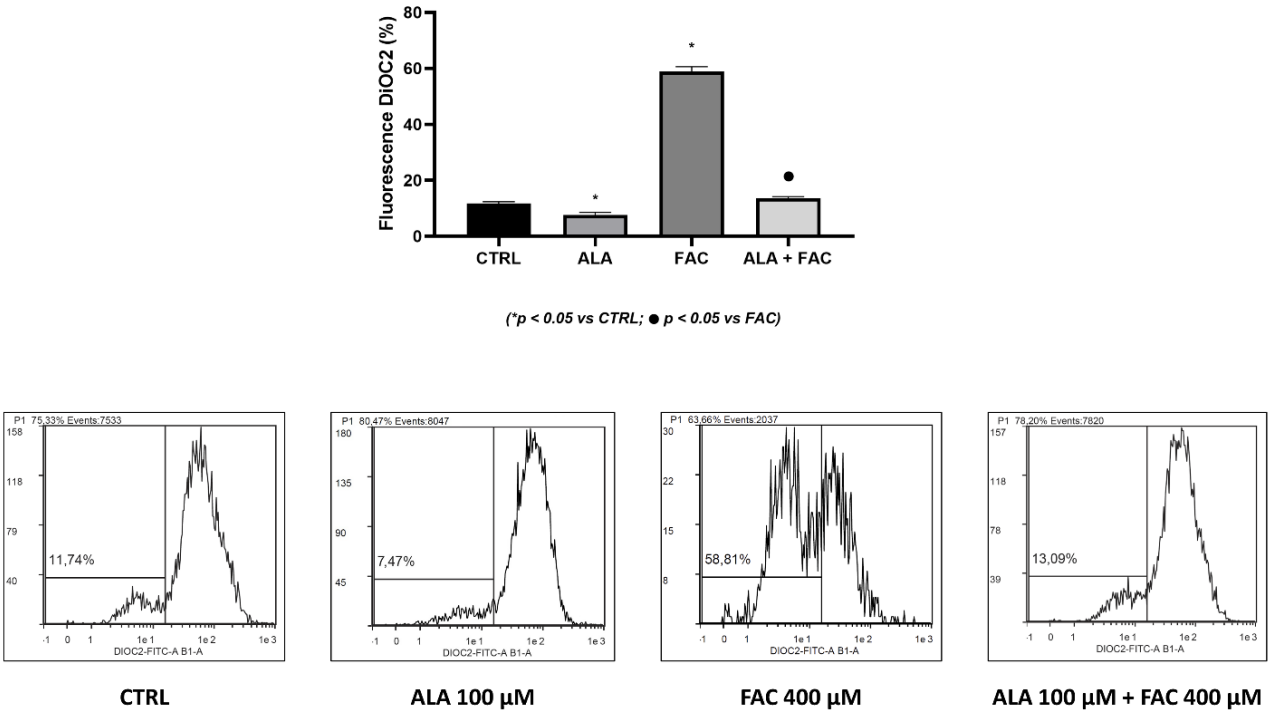

Figure 10. Evaluation of mitochondrial membrane potential by flow cytometry (DiOC2). HMC3 cells were pre-treated with ALA 100 µM (3h), then treated with FAC 400 µM (24h).

3.5 Iron promotes mitochondrial biogenesis

Changes in mitochondrial mass were evaluated by flow cytometry using MitoTracker probe. Figure 11 shows an increase of mitochondrial content in presence of FAC, while the pre-treatment with ALA reduced the same parameter. In opposite, the single treatment with ALA did not cause change in mitochondrial mass, showing levels of mitochondrial content comparable to control.

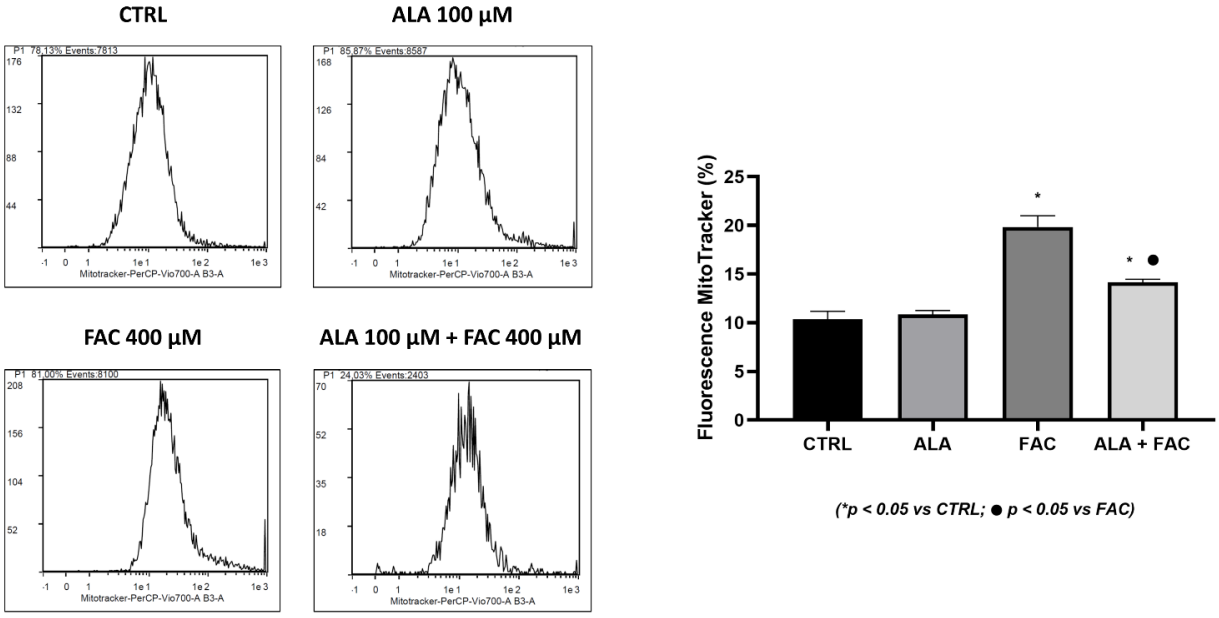

Figure 11. Evaluation of mitochondrial mass content by flow cytometry (MitoTracker). HMC3 cells were pre-treated with ALA 100 µM (3h), then treated with FAC 400 µM (24h).

As shown in Figure 12, iron overload caused the over expression of genes related to mitochondrial biogenesis. In particular, treatment with FAC led to an increase of ATP Synthase F1 Subunit Beta (ATP5B, Fig 12A), NADH ubiquinone oxidoreductase subunit S4 (NDUFS4, Fig 12B), Cytochrome B (CYTB, Fig 12C) and mitochondrial transcription factor A (TFAM, Fig 12D) levels. If, on one hand, the ALA treatment alone did not affect the modulation of those genes, on the other, the combined presence with FAC reverted the effect caused by iron overload.

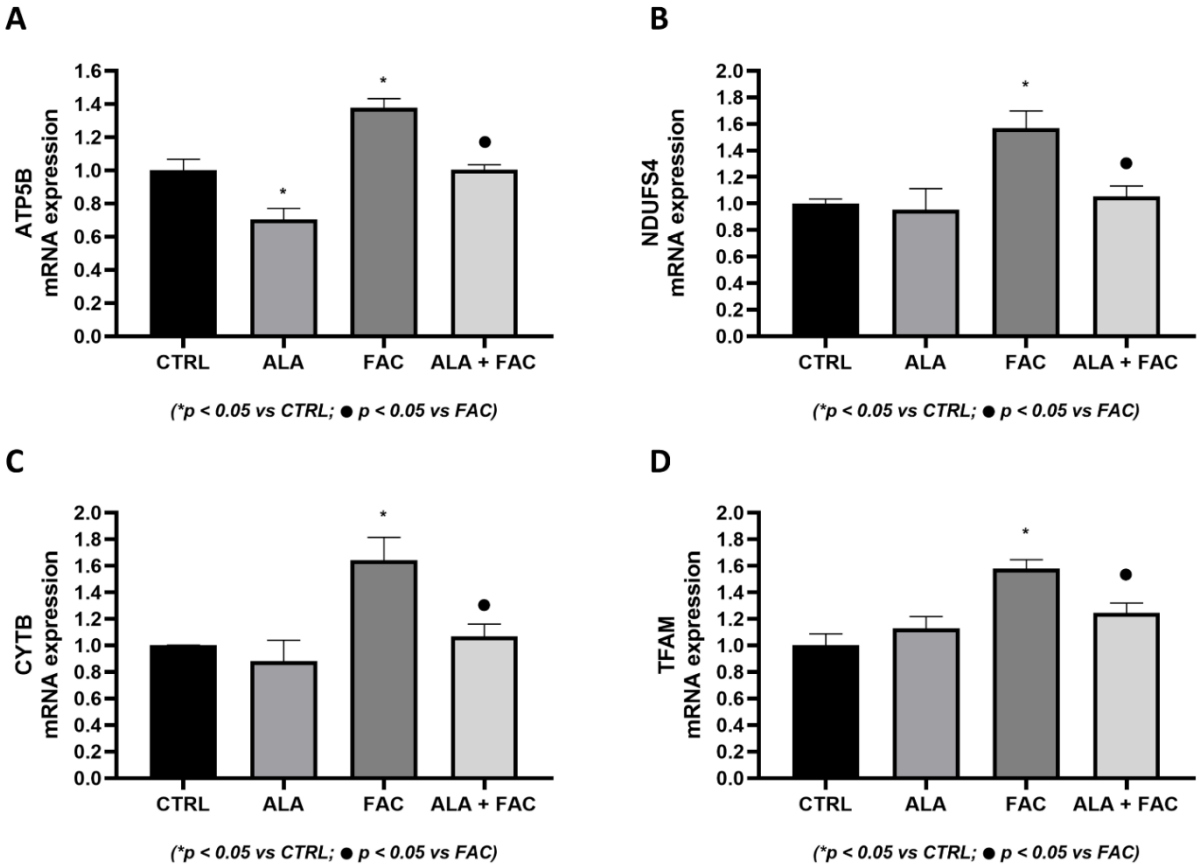

Figure 12. Gene expression of ATP5B, NDUFS4, CYTB and TFAM. HMC3 cells were pre-treated with ALA 100 µM (3h), then treated with FAC 400 µM (6h).

3.6 Iron overload enhances ROS production

The quantitative measurement of cells undergoing oxidative stress and ROS production was evaluated by flow cytometry. Treatment with FAC led to a strong increase of ROS production in HMC3 cells, compared to the other groups. On the other hand, iron overload in presence of ALA was not able to induce the same amount of ROS content, showing a level of ROS production slightly higher than control group (Figure 13).

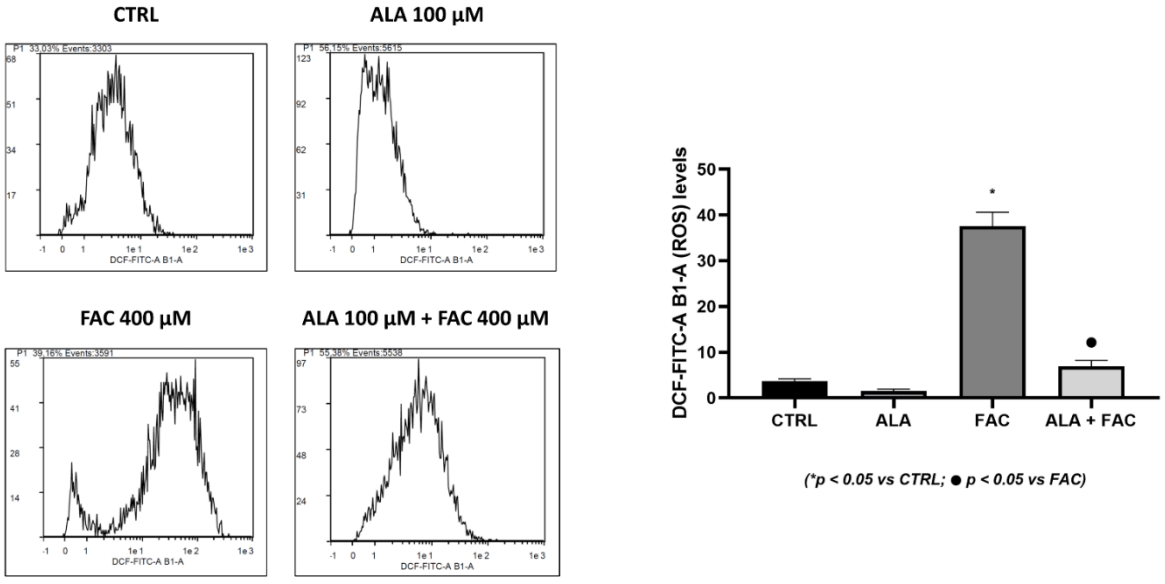

Figure 13. Analysis of ROS production by flow cytometry. HMC3 cells were pre-treated with ALA 100 µM (3h), then treated with FAC 400 µM (24h).

3.7 ALA restores GSH levels

According to data obtained in ROS analysis, pre-treatment with ALA was able to regulate the oxidative stress condition by enhancing GSH levels, both in presence and in absence of iron overload, despite the single treatment with FAC significantly affected the GSH content compared to untreated cells (Figure 14).

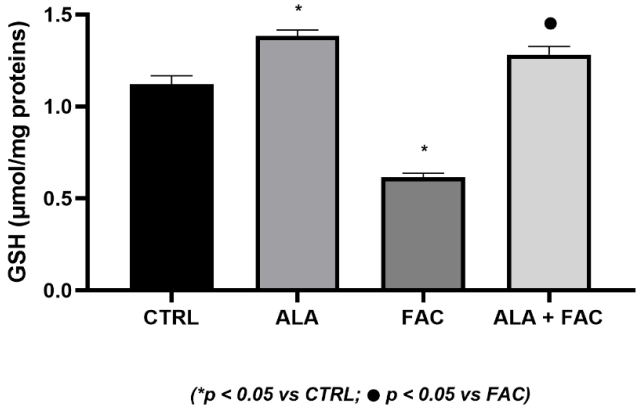

Figure 14. Evaluation of GSH levels. HMC3 cells were pre-treated with ALA 100 µM (3h), then treated with FAC 400 µM (24h).

3.8 Iron overload and inflammation

As shown by Figure 15A, 15B, 15C, the 6h exposure to iron was able to induce the gene expression of markers closely related to inflammation, such as prostaglandin-endoperoxide synthase (COX-2) and interleukins (IL-6, IL-1β). Due to the pre-treatment with ALA, the expression of such genes was reduced to control level. On the other hand, as shown by Figure 15D, although TNF-α levels were not affected by FAC (6h), ALA was still able to decrease the gene expression of the cytokine, both in presence and absence of FAC, compared to control.

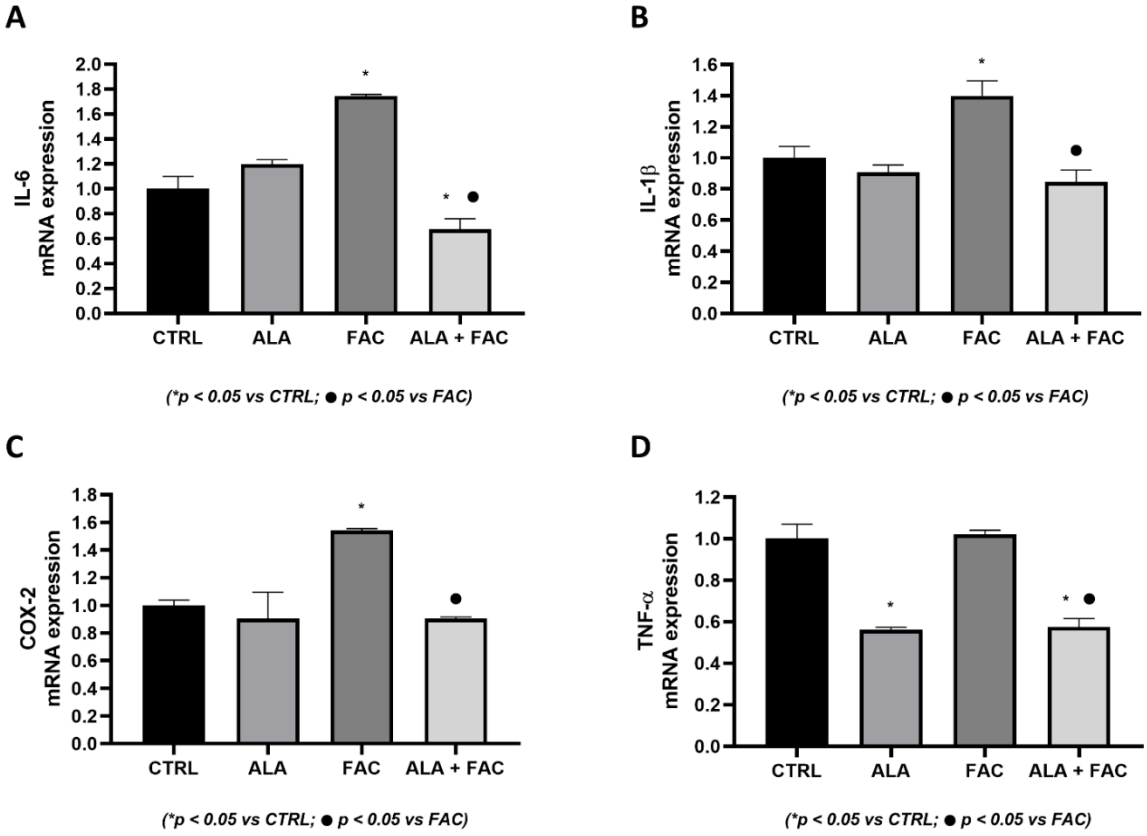

Figure 15. Gene expression of inflammation markers (IL-6, IL-1β, COX-2, TNF-α). HMC3 cells were pre-treated with ALA 100 µM (3h), then treated with FAC 400 µM (6h).

In order to investigate the behavior of inflammation markers in presence of iron overload at a different time point, gene expression was evaluated after 24h. Contrary to what is shown in Figure 15D, a longer exposure to FAC significantly affected the gene expression of TNF-α (Figure 16A). Despite this change, ALA + FAC group maintained a strong reduction of TNF-α levels, even lower than control. On the other hand, following an opposite behavior, FAC (24h) did not significantly affect IL-1β gene expression (Figure 16B), in contrast to what is shown at a different time point (6h) (Figure 15B). Nevertheless, ALA pre-treatment was able to reduce the basal level of IL-1β compared to untreated cells.

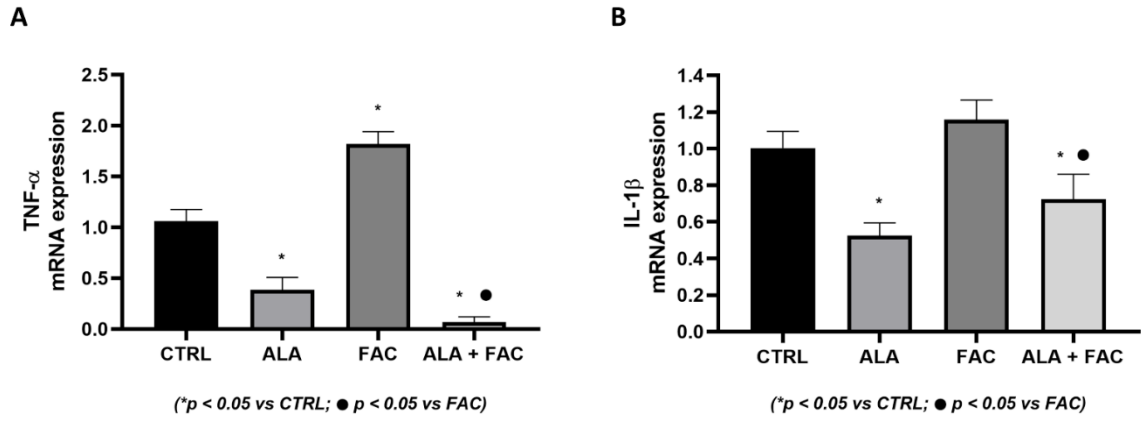

Figure 16. Gene expression of TNF-α and IL-1β. HMC3 cells were pre-treated with ALA 100 µM (3h), then treated with FAC 400 µM (24h).

The protein level of IL-6 was evaluated in conditioned media after treatments (Figure 17). Cells treated with FAC for 24h released a higher level of IL-6 compared to the other groups, while the presence of ALA was able to reduce the IL-6 content in the medium both alone and in combination with FAC.

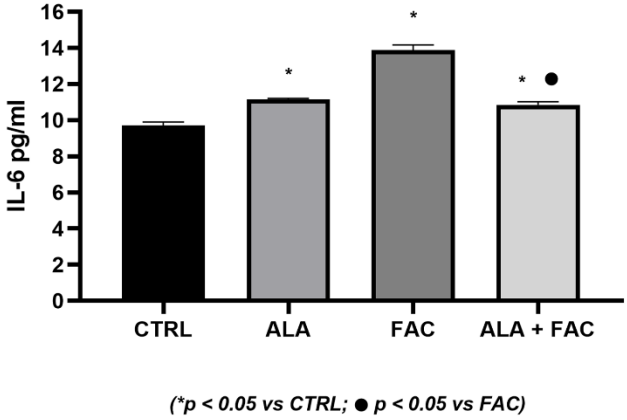

Figure 17. Protein expression of IL-6 by ELISA kit. HMC3 cells were pre-treated with ALA 100 µM (3h), then treated with FAC 400 µM (24h).

3.9 ALA reverts M1/M2 switch in microglia

The M1/M2 phenotype in microglia is characterized by over expression of iNOS (NOS2) or Arginase 1 (ARG1), respectively. Comparing the expression of the two enzymes involved in the arginine metabolism, the immunofluorescence assay (Figure 18) shows that the single treatment with ALA did not upregulate NOS2 protein expression, while ARG1 levels were visibly enhanced. Following an opposite behavior, the inflammatory condition due to the FAC treatment caused a strong over-expression of NOS2, data confirmed by the significantly reduced expression of ARG1. Finally, the pre-treatment with ALA rescued the effects led by iron overload: the expression of NOS2 was sensibly reduced compared to FAC group, whereas the increased level of ARG1 showed the anti-inflammatory profile of M2 microglia.

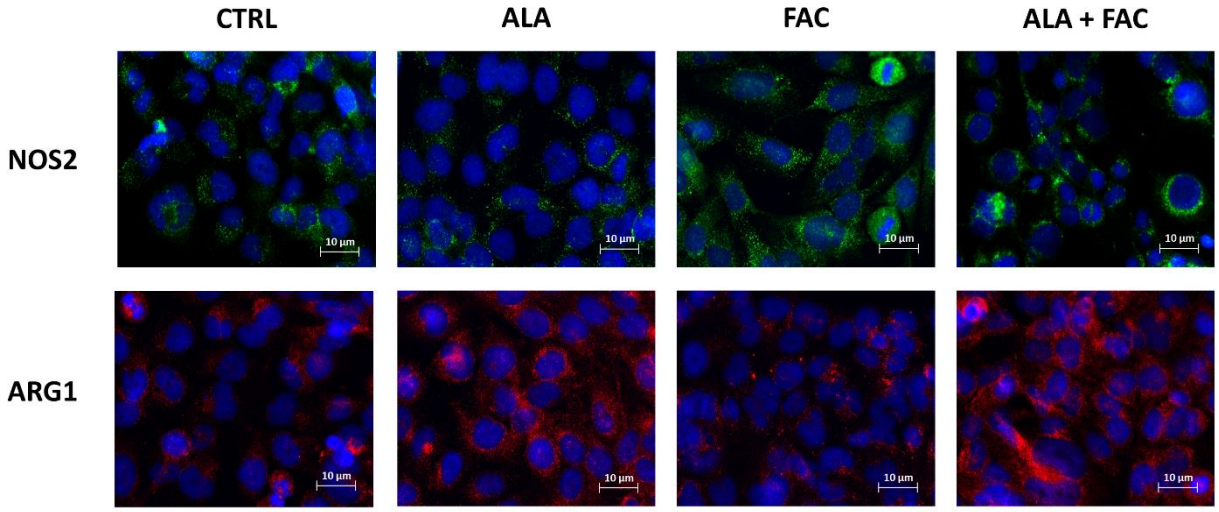

Figure 18. Evaluation of NOS2 and ARG1 expression by immunofluorescence (Scale Bar: 10 µm). HMC3 cells were pre-treated with ALA 100 µM (3h), then treated with FAC 400 µM (24h).

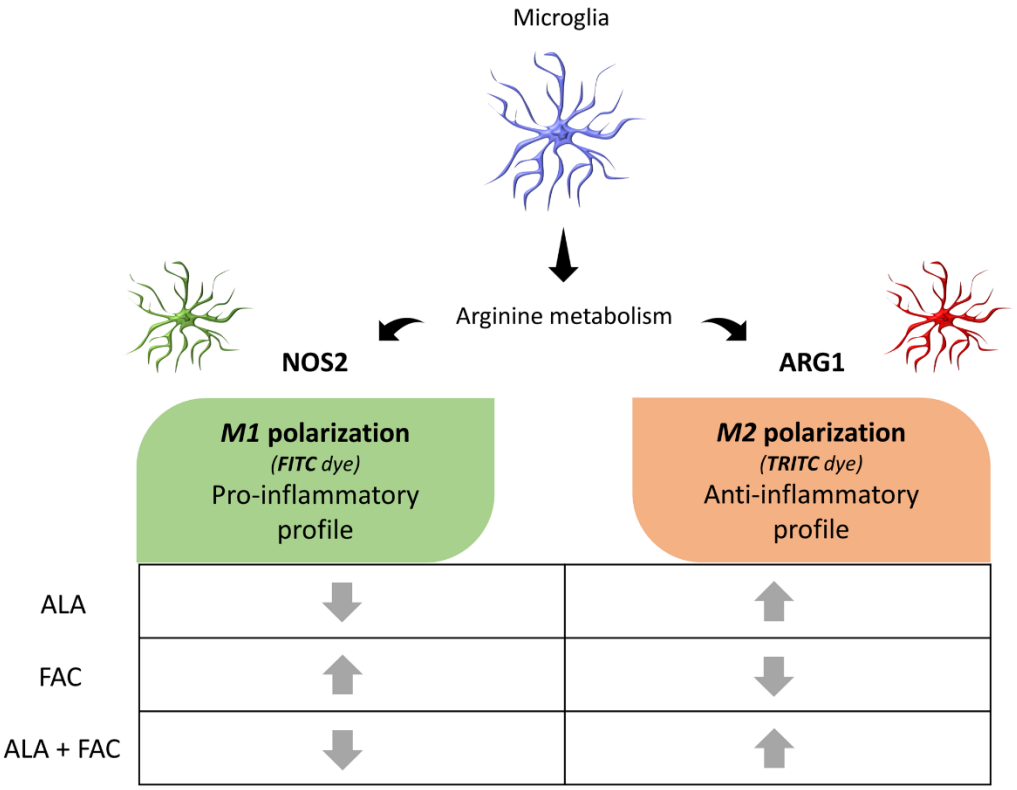

Figure 19. Schematic description of microglial polarization after treatment with ALA and FAC.

3.10 ALA chelating properties In Vivo

As shown by Perls assay (Figure 20), FAC treatment (60h) in a zebrafish *in vivo* model resulted in a significant increase in brain iron storage when compared to control. The following administration of ALA, after 60h of iron exposure, reduced the iron content to levels comparable to the untreated sample.

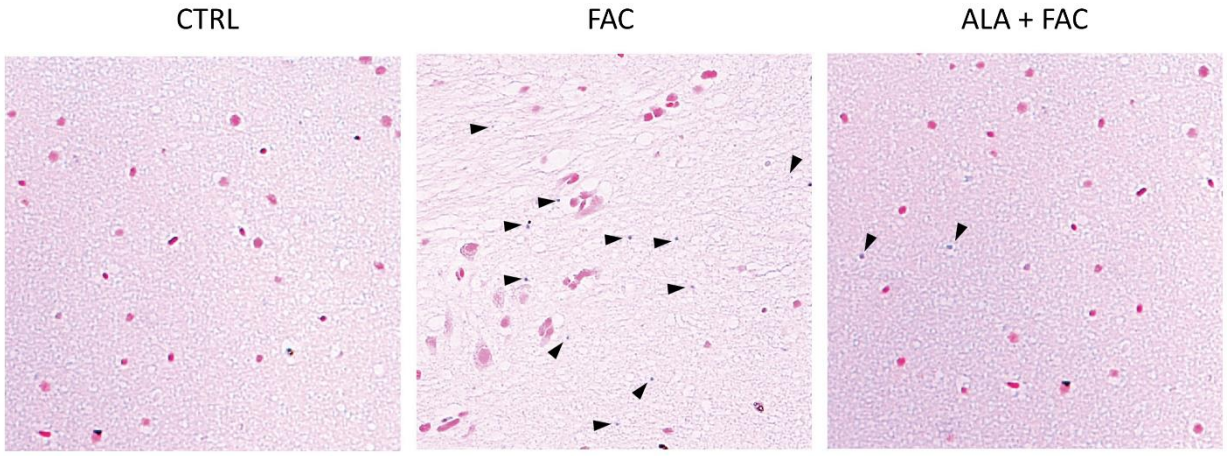

Figure 20. Iron storage in zebrafish brain tissue (immunohistochemical Perls assay). Zebrafish were pre-treated with FAC 400 µM (60h), then treated with ALA 100 µM (60h).

3.11 ALA reduces microglia activation In Vivo

In order to evaluate the microglia activation in response to the neuroinflammation induced by FAC, glial fibrillary acidic protein (GFAP) levels were detected in zebrafish brain (Figure 21). Iron overload induced by FAC led to a marked overexpression of GFAP compared to control, while the single treatment with ALA did not affect physiological GFAP levels. Interestingly, ALA post-treatment following iron overload was able to control microglia activation by significantly reducing GFAP expression compared to FAC sample.

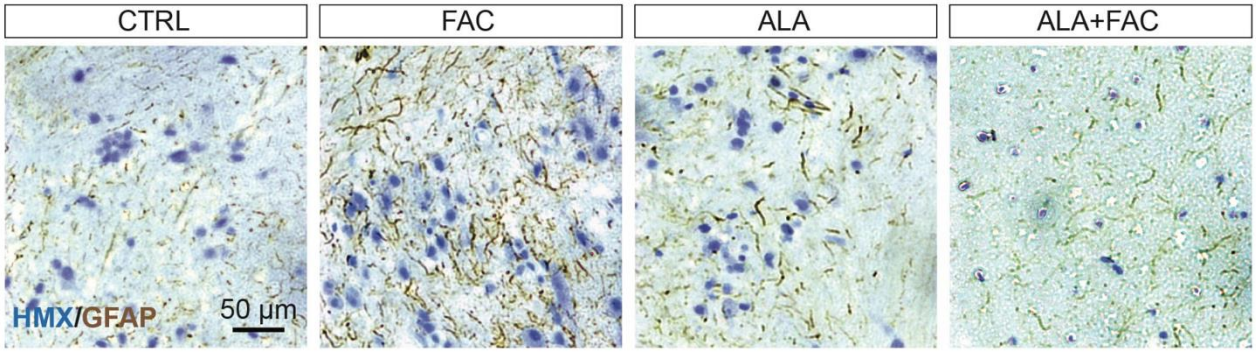

Figure 21. GFAP expression in zebrafish brain tissue (immunohistochemical assay). Zebrafish were pre-treated with FAC 400 µM (60h), then treated with ALA 100 µM (60h).

3.12 Oxidative stress and inflammation in Zebrafish brain

Zebrafish brain lysates were collected in order to observe expression changes of genes related to oxidative stress and inflammation after treatment with FAC. Figure 22 shows a marked increase of HO-1 (hmox1b), SOD-1 (sod1) and COX-1 (ptgs1) levels following iron overload. Despite the strong stress condition caused by FAC, the subsequent administration of ALA was able to reduce genes expression of all markers to control level.

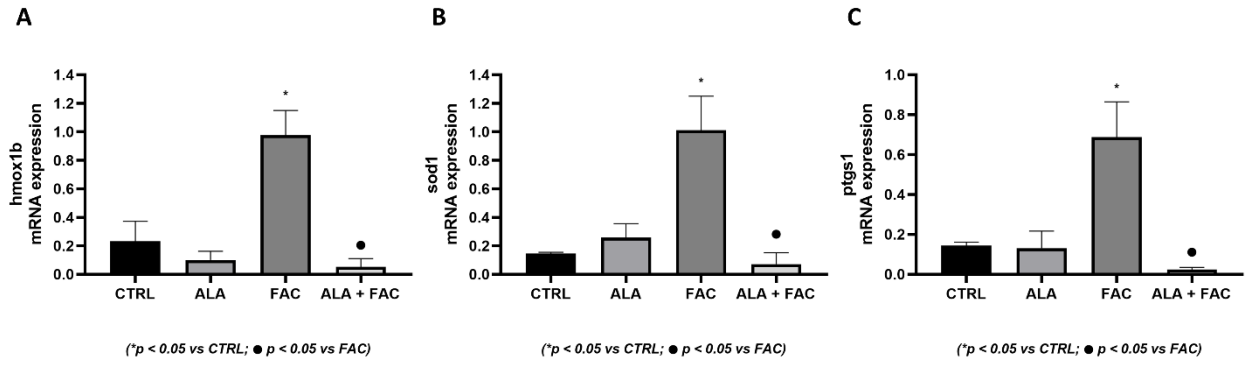

Figure 22. Gene expression of hmox1b, sod1, ptgs1. Zebrafish were pre-treated with FAC 400 µM (60h), then treated with ALA 100 µM (60h).

4. Discussion

Iron is a crucial nutrient for multiple biological functions, including oxygen and electron transport, redox reactions, cell division, nucleotide synthesis and myelination [101]. In the brain, iron homeostasis plays a key role in the maintenance of physiological functions, thus a dysregulation can lead to serious neurodegenerative diseases, such as Alzheimer's disease and Parkinson's disease [102, 103]. Despite metal homeostasis is a well-known focus to approach in these kinds of brain diseases, the role of iron accumulation following ICH or traumatic brain injury has yet to be fully determined. Both conditions are broadly defined as bleeding within the cranium, leading to different brain injuries categorized by severity and prognosis. It is known that iron liberation into brain tissue occurs 24h after hemorrhage, while the accumulation into perihematomal tissue is evident within few days after ICH: for this reason, the early resort to surgical or pharmacological methods is essential to face iron overload and iron related secondary injury. Few chelating agents approved by the US Food and Drug Administration (FDA) are currently available for this purpose. Among them, Deferoxamine is the most used as iron chelator, and few evidences suggest the use of this drug for its neuroprotective role in ICH condition, with the ability to prevent neural damage and to reduce perihematomal edema occurring [104-107]. On the other hand, insufficient evidence exists to determine the effect of Deferoxamine on neurologic outcomes after ICH and the safety of this intervention, furthermore the prolonged administration is associated to neurotoxicity [108-110]. Indeed, beyond ICH, iron overload affecting brain functionalities may occur under various and collateral pathological conditions, including genetic forms, such as hereditary haemochromatosis, or those acquired forms that require lifelong regular blood transfusions, such as thalassemia [111-113]. In these conditions, more than 10% of patients undergoing therapy with Deferoxamine experience several adverse effects, such as retinal and auditory

neurotoxicity, neutropenia and agranulocytosis, diarrhea, headache, nausea, abdominal pain, increased serum creatinine, and increased liver enzymes, rash, fatigue, and arthralgia [114]. In order to find an alternative therapy capable to exert the same efficacy of classic chelating drugs on ICH-like condition avoiding though the rise of such side effects, ALA properties were assessed both in *in vitro* and *in vivo* brain models of iron overload. It is well-known that iron accumulation is able to affect microglia proliferation and viability, leading to an overall degeneration of functionalities [115-117]. Our results on *in vitro* model confirmed that by showing a strong reduction of cell proliferation after treatment with FAC, that was also able to influence the apoptotic rate of microglia cells. Indeed, FAC led to intracellular iron accumulation, showed by increased levels of FPN1 and DMT1, thus resulting in a significant impairment of mitochondrial membrane potential, thereby causing increasing rate of ROS generation and cell suffering. Our results showed that pre-treatment with ALA prevented FAC toxicity by protecting cells both as iron chelator and as anti-oxidant: on one hand, ALA treatment reduced the expression of iron transporters FPN1 and DMT1, due to the lower iron absorption by the cell; on the other, ALA alleviated oxidative stress both enzymatically and by a free radical direct scavenging effect [118, 119]. ALA is a dithiol compound normally bound to lysine residues of mitochondrial α-keto acid dehydrogenases, which reduce ALA to dihydrolipoic acid (DHLA), which is known for its strong antioxidant properties [120]. The presence of ALA maintained the levels of ROS at basal conditions in microglia, reducing iron content and restoring mitochondrial membrane potential and integrity. Our results were further confirmed by changes both in intracellular GSH content and in HO-1 expression. The GSH system is the main cellular defense mechanism regulating the intracellular redox state and its synthesis is promptly activated by various oxidative triggers [121]. Under physiological conditions, the reduced GSH is the major form available with its concentration from 10 to 100-

folds higher than the oxidized species, which guarantees the control on oxidative balance [122]. Our results showed that treatment with FAC decreased the available amount of reduced GSH, while the pre-treatment with ALA enhanced the antioxidant defenses for the cells by restoring GSH content. In parallel, results showed that HO-1, an NRF2 regulated protein involved in redox balance, is strongly upregulated following FAC treatment. As mentioned before, HO-1 is the enzyme responsible for degradation of endogenous iron protoporphyrin Heme; it catalyzes the reaction's rate-limiting step, producing ferrous ions, carbon monoxide, and biliverdin, whose reduction is operated by biliverdin reductase, resulting in bilirubin formation [123]. HO-1 plays a pivotal role in regulating redox homeostasis in virtue of its anti-inflammatory, antioxidant and anti-apoptotic properties. It has been reported that the activation of HO-1 is a ubiquitous cellular response to oxidative stress: HO-1 activation stimulates ferritin synthesis, which ultimately contributes to iron detoxification [124, 125]. Basing on that, results suggest that iron overload in microglia triggered the activation of cellular defenses trough upregulation of HO-1, while the co-presence of ALA was able to avoid the activation of this pathway, probably due to the management of GSH content. As shown, the stress condition caused by FAC affected mitochondrial functions and homeostasis through the impairment of the membrane potential. According to Hoeft et al., macrophage cells exposed to iron overload enhanced mitochondrial mass, increasing the proportion of nonfunctional mitochondria relative to total mitochondria. Basing on their results, authors suggested that mitochondrial mass can be increased by promoting mitochondrial biogenesis and/or by decreasing mitophagy, and reported that treating cells with a combination of lipopolysaccharide (LPS) and iron (as further source of stress), increased mRNA levels of genes involved in mitochondrial biogenesis [126]. Furthermore, different works have shown that, despite the total mitochondrial mass is augmented, damaged or nonfunctional mitochondria

produce more ROS [127, 128]. Our results largely confirmed the suggestion reported: iron overload in microglia led to an increase of total mitochondrial mass, although new mitochondria demonstrated an unfunctional behavior, as shown by abnormal ROS production and by depolarization of mitochondrial membrane. Moreover, treatment with FAC affected mitochondrial biogenesis by increasing related genes levels, such as ATP5B, NDUFS4, CYTB and TFAM. In particular, mitochondrial biogenesis process is regulated by nuclear transcription factors, such as NRF1 and NRF2, and the coactivator peroxisome proliferator-activated receptor γ coactivator 1 (PGC1α), which upregulates expression of TFAM, enabling replication of mitochondrial DNA [129-131]. Following our results, we can speculate that oxidative stress caused by iron overload is able to activate HO-1 expression as well as to affect mitochondrial biogenesis probably through a shared signaling pathway, involving nuclear translocation of NRF2 and binding to antioxidant response elements in the nuclear DNA. Moreover, although ATP5B, NDUFS4 and CYTB are commonly associated to the respiratory chain functions and the oxidative phosphorylation system, an increase of their total level in microglia following iron-induced oxidative stress is not related to the cell metabolic switch, but to the enhanced number of new mitochondria [132]. The ALA pre-administration reverted the affection of FAC on mitochondria probably by exerting an antioxidant effect via NRF2/HO-1 pathway, thus restoring basal levels of mitochondrial biogenesis rate [133]. Iron and inflammation are intertwined in a bidirectional relationship, in which iron modifies the inflammatory phenotype of microglia and infiltrating macrophages, and in turn, these cells secrete diffusible mediators that reshape neuronal iron homeostasis and regulate iron entry into the brain. Our results showed that even a brief exposure to iron is able to rise an inflammatory condition in microglia cells: behaving as M1 type cells, microglia over-expressed different pro-inflammatory cytokines and inflammation-related markers, including IL-6, IL-1β

and COX-2. Moreover, after a longer exposure to FAC, microglia enhanced the expression of TNF-α and allowed the secretion of IL-6 protein. The strong affection of iron overload on M1 microglia polarization was also confirmed by the over expression of the related main marker NOS2. Interestingly, pre-treatment with ALA prevented the inflammatory state not only by reducing pro-inflammatory cytokines expression, but also counteracting the NOS2 expression, and probably limiting the switch to M1 type, by enhancing ARG1 levels, known marker of anti-inflammatory M2 type cell. Our results confirmed what shown by Su Min Kim et al.: in their paper, authors demonstrated that ALA was able to reduce M1 phenotype markers expression following LPS stimulation in BV2 microglial cells, whereas the M2 phenotype markers levels were significantly enhanced. They suggested that treatment with ALA could revert the inflammatory condition led by LPS stimulation by promoting M1 microglia switch toward M2 phenotype [134]. Our results obtained *in vitro* demonstrated that pre-treatment with ALA is able to strengthen microglia cells by protecting them from the toxicity led by iron overload. However, since ICH and the subsequent iron accumulation can be commonly considered unpredictable events, pre-administration of ALA used in *in vitro* model can only give conceptual answers, but cannot completely overlap to the clinical condition, in which the therapy is allowed only after ICH occurring. For this reason, in order to test ALA efficacy in a translational model, we developed an *in vivo* iron overload model based on acute exposure of zebrafish to FAC (less than 90 hours), administrating ALA only after iron accumulation. Zebrafish is an important vertebrate model used in research due to its combination of excellent embryology and genetic manipulation. It has been shown that the uptake of iron in zebrafish is via absorption from the water across the gill membrane and intestinal mucosa [135]. Due to this mechanism, there is the possibility for iron to be lost through the gills by diffusion following concentration gradient, for instance when zebrafish are transferred to a

media with a lower concentration of iron [136]. In order to ensure that every change in iron content or in gene expression was due to ALA efficacy as iron chelator and antioxidant, the media in the FAC group was replaced with untreated water in parallel with media replacement in ALA+FAC group, as shown by scheme in Figure 6. Obtained data demonstrated that post-administrated ALA is able to strongly reduce the iron content accumulated in the brain. It has been reported that pro-inflammatory stimuli, including LPS and IFN-γ, are associated to increased expression of GFAP, which represents astroglial activation and gliosis during neurodegeneration [137]. Increased levels of GFAP have been found at the periphery of ischemic lesions after neurodegenerative insults, and are associated with senile plaques, well known pathological markers of Alzheimer's disease [138, 139]. Moreover, the measure of GFAP levels is considered proportional to the severity of astroglial activation [140, 141]. Afterwards, astrocytes activation regulates microglial responses following immune challenge represented by external stimuli or neuroinflammation in brain: in this regard, both microglia and astrocytes contribute to the control of inflammatory acute phase and regulate immune response in brain. Similar to assessing microglial activation by morphology, activation states of astrocytes are determined based on increased GFAP labeling [142]. Our results showed that iron overload is able to significantly increase GFAP expression in zebrafish brain, that represents astroglial activation after neuroinflammation induced by FAC. The recent paper published by Memudu and Adanike demonstrated that ALA can control inflammatory conditions thereby downregulating the process of cognitive impairment via its ability to induce neuroprotection through synergistic interaction with astrocytes. In their results, ALA protects astrocytes repairing and synaptogenesis from scopolamine invoked oxidative stress, via reduction of GFAP levels [143]. Moreover, several studies suggested that ALA mechanisms of neuroprotection could be linked with the mitochondrial functionality and the increase of

intracellular levels of GSH, which helps to reduce the migration of lymphocytes, monocytes, and other pro-inflammatory cytokines into the brain, which ultimately results in the inhibition of reactive astrocytes [144-148]. According to these studies, our results showed that ALA post-treatment completely reverts GFAP over-expression led by iron overload, suggesting a significant efficacy on astroglial activation control. Furthermore, because of its direct and indirect antioxidant properties and the efficacy on inflammatory conditions, ALA resulted in a significant reduction of hmox1b, sod1, ptgs1 genes expression in the brain when compared to FAC treatment. Therefore, our results are consistent with those obtained by Camiolo et al., in which they proved the efficacy of ALA on iron storage reduction in zebrafish liver and intestine, known as the main tissues involved in iron absorption [92]. With our new data, we demonstrated that ALA is able to exert its activity as iron chelator reaching the brain tissue, without showing any loss of effectiveness on iron overload.

5. Conclusions

ICH is a devastating condition whereby a hematoma is formed with or without blood extension into the ventricles. After ICH, erythrocytes are released into the brain parenchyma, where they lyse within hours/days, releasing their components, including hemoglobin, into the extracellular space. While the iron homeostatic mechanism is tightly regulated in physiological conditions, the amount of hemoglobin released may overwhelm this iron-handling system. The following iron overload represents a critical cause of several harmful reactions for brain tissue. With our results we demonstrated that ALA, a natural compound widely tolerate by microglia cells and brain tissue, can exert its antioxidant, anti-inflammatory and iron-chelating properties both *in vitro* and *in vivo*. Since there are still many questions regarding reliable therapies available to face ICH-following iron overload, we suggest that ALA could be considered, in the next future, as a new alternative choice to approach this kind of clinical issue, especially for the absence of side effects risen after its use.

6. References

1. van Asch, C. J.; Luitse, M. J.; Rinkel, G. J.; van der Tweel, I.; Algra, A.; Klijn, C. J., Incidence, case fatality, and functional outcome of intracerebral haemorrhage over time, according to age, sex, and ethnic origin: a systematic review and meta-analysis. *Lancet Neurol* **2010,** 9, (2), 167-76.
2. Bako, A. T.; Pan, A.; Potter, T.; Tannous, J.; Johnson, C.; Baig, E.; Meeks, J.; Woo, D.; Vahidy, F. S., Contemporary Trends in the Nationwide Incidence of Primary Intracerebral Hemorrhage. *Stroke* **2022,** 53, (3), e70-e74.
3. Aguilar, M. I.; Freeman, W. D., Spontaneous intracerebral hemorrhage. *Semin Neurol* **2010,** 30, (5), 555-64.
4. Greenberg, S. M.; Vernooij, M. W.; Cordonnier, C.; Viswanathan, A.; Al-Shahi Salman, R.; Warach, S.; Launer, L. J.; Van Buchem, M. A.; Breteler, M. M.; Microbleed Study, G., Cerebral microbleeds: a guide to detection and interpretation. *Lancet Neurol* **2009,** 8, (2), 165-74.
5. Dye, J. A.; Rees, G.; Yang, I.; Vespa, P. M.; Martin, N. A.; Vinters, H. V., Neuropathologic analysis of hematomas evacuated from patients with spontaneous intracerebral hemorrhage. *Neuropathology* **2014,** 34, (3), 253-60.
6. Wilkinson, D. A.; Pandey, A. S.; Thompson, B. G.; Keep, R. F.; Hua, Y.; Xi, G., Injury mechanisms in acute intracerebral hemorrhage. *Neuropharmacology* **2018,** 134, (Pt B), 240-248.
7. Ziai, W. C.; Carhuapoma, J. R., Intracerebral Hemorrhage. *Continuum (Minneap Minn)* **2018,** 24, (6), 1603-1622.
8. Garton, T.; Keep, R. F.; Hua, Y.; Xi, G., Brain iron overload following intracranial haemorrhage. *Stroke Vasc Neurol* **2016,** 1, (4), 172-184.
9. Keep, R. F.; Hua, Y.; Xi, G., Intracerebral haemorrhage: mechanisms of injury and therapeutic targets. *Lancet Neurol* **2012,** 11, (8), 720-31.
10. Mendelow, A. D.; Gregson, B. A.; Fernandes, H. M.; Murray, G. D.; Teasdale, G. M.; Hope, D. T.; Karimi, A.; Shaw, M. D.; Barer, D. H.; investigators, S., Early surgery versus initial conservative treatment in patients with spontaneous supratentorial intracerebral haematomas in the International Surgical Trial in Intracerebral Haemorrhage (STICH): a randomised trial. *Lancet* **2005,** 365, (9457), 387-97.
11. Morgenstern, L. B.; Demchuk, A. M.; Kim, D. H.; Frankowski, R. F.; Grotta, J. C., Rebleeding leads to poor outcome in ultra-early craniotomy for intracerebral hemorrhage. *Neurology* **2001,** 56, (10), 1294-9.
12. Imberti, R.; Pietrobono, L.; Klersy, C.; Gamba, G.; Iotti, G. A.; Cornara, G., Intraoperative intravenous administration of rFVIIa and hematoma volume after early surgery for spontaneous intracerebral hemorrhage: a randomized prospective phase II study. *Minerva Anestesiol* **2012,** 78, (2), 168-75.
13. Beez, T.; Steiger, H. J.; Etminan, N., Pharmacological targeting of secondary brain damage following ischemic or hemorrhagic stroke, traumatic brain injury, and bacterial meningitis - a systematic review and meta-analysis. *BMC Neurol* **2017,** 17, (1), 209.
14. Wu, J.; Hua, Y.; Keep, R. F.; Nakamura, T.; Hoff, J. T.; Xi, G., Iron and iron-handling proteins in the brain after intracerebral hemorrhage. *Stroke* **2003,** 34, (12), 2964-9.

15. Zhao, F.; Hua, Y.; He, Y.; Keep, R. F.; Xi, G., Minocycline-induced attenuation of iron overload and brain injury after experimental intracerebral hemorrhage. *Stroke* **2011,** 42, (12), 3587-93.
16. Selim, M.; Yeatts, S.; Goldstein, J. N.; Gomes, J.; Greenberg, S.; Morgenstern, L. B.; Schlaug, G.; Torbey, M.; Waldman, B.; Xi, G.; Palesch, Y., Deferoxamine Mesylate in Intracerebral Hemorrhage, I., Safety and tolerability of deferoxamine mesylate in patients with acute intracerebral hemorrhage. *Stroke* **2011,** 42, (11), 3067-74.
17. Xiong, X. Y.; Wang, J.; Qian, Z. M.; Yang, Q. W., Iron and intracerebral hemorrhage: from mechanism to translation. *Transl Stroke Res* **2014,** 5, (4), 429-41.
18. Chang, E. F.; Claus, C. P.; Vreman, H. J.; Wong, R. J.; Noble-Haeusslein, L. J., Heme regulation in traumatic brain injury: relevance to the adult and developing brain. *J Cereb Blood Flow Metab* **2005,** 25, (11), 1401-17.
19. Madangarli, N.; Bonsack, F.; Dasari, R.; Sukumari-Ramesh, S., Intracerebral Hemorrhage: Blood Components and Neurotoxicity. *Brain Sci* **2019,** 9, (11).
20. Wagner, K. R.; Sharp, F. R.; Ardizzone, T. D.; Lu, A.; Clark, J. F., Heme and iron metabolism: role in cerebral hemorrhage. *J Cereb Blood Flow Metab* **2003,** 23, (6), 629-52.
21. Connor, J. R.; Menzies, S. L.; Burdo, J. R.; Boyer, P. J., Iron and iron management proteins in neurobiology. *Pediatr Neurol* **2001,** 25, (2), 118-29.
22. Singh, N.; Haldar, S.; Tripathi, A. K.; Horback, K.; Wong, J.; Sharma, D.; Beserra, A.; Suda, S.; Anbalagan, C.; Dev, S.; Mukhopadhyay, C. K.; Singh, A., Brain iron homeostasis: from molecular mechanisms to clinical significance and therapeutic opportunities. *Antioxid Redox Signal* **2014,** 20, (8), 1324-63.
23. Murray-Kolb, L. E., Iron and brain functions. *Curr Opin Clin Nutr Metab Care* **2013,** 16, (6), 703-7.
24. Ke, Y.; Qian, Z. M., Brain iron metabolism: neurobiology and neurochemistry. *Prog Neurobiol* **2007,** 83, (3), 149-73.
25. Arosio, P.; Carmona, F.; Gozzelino, R.; Maccarinelli, F.; Poli, M., The importance of eukaryotic ferritins in iron handling and cytoprotection. *Biochem J* **2015,** 472, (1), 1-15.
26. McCarthy, R. C.; Kosman, D. J., Mechanisms and regulation of iron trafficking across the capillary endothelial cells of the blood-brain barrier. *Front Mol Neurosci* **2015,** 8, 31.
27. Benarroch, E. E., Brain iron homeostasis and neurodegenerative disease. *Neurology* **2009,** 72, (16), 1436-40.
28. Gaasch, J. A.; Lockman, P. R.; Geldenhuys, W. J.; Allen, D. D.; Van der Schyf, C. J., Brain iron toxicity: differential responses of astrocytes, neurons, and endothelial cells. *Neurochem Res* **2007,** 32, (7), 1196-208.
29. Ayer, R. E.; Zhang, J. H., Oxidative stress in subarachnoid haemorrhage: significance in acute brain injury and vasospasm. *Acta Neurochir Suppl* **2008,** 104, 33-41.
30. Welch, K. D.; Davis, T. Z.; Van Eden, M. E.; Aust, S. D., Deleterious iron-mediated oxidation of biomolecules. *Free Radic Biol Med* **2002,** 32, (7), 577-83.
31. Bai, Q.; Liu, J.; Wang, G., Ferroptosis, a Regulated Neuronal Cell Death Type After Intracerebral Hemorrhage. *Front Cell Neurosci* **2020,** 14, 591874.
32. Imai, T.; Iwata, S.; Hirayama, T.; Nagasawa, H.; Nakamura, S.; Shimazawa, M.; Hara, H., Intracellular Fe(2+) accumulation in endothelial cells and pericytes induces blood-

brain barrier dysfunction in secondary brain injury after brain hemorrhage. *Sci Rep* **2019,** 9, (1), 6228.
33. Zhang, Y.; Khan, S.; Liu, Y.; Zhang, R.; Li, H.; Wu, G.; Tang, Z.; Xue, M.; Yong, V. W., Modes of Brain Cell Death Following Intracerebral Hemorrhage. *Front Cell Neurosci* **2022,** 16, 799753.
34. Qu, J.; Chen, W.; Hu, R.; Feng, H., The Injury and Therapy of Reactive Oxygen Species in Intracerebral Hemorrhage Looking at Mitochondria. *Oxid Med Cell Longev* **2016,** 2016, 2592935.
35. Wu, M.; Gao, R.; Dang, B.; Chen, G., The Blood Component Iron Causes Neuronal Apoptosis Following Intracerebral Hemorrhage via the PERK Pathway. *Front Neurol* **2020,** 11, 588548.
36. Levy, Y. S.; Streifler, J. Y.; Panet, H.; Melamed, E.; Offen, D., Hemin-induced apoptosis in PC12 and neuroblastoma cells: implications for local neuronal death associated with intracerebral hemorrhage. *Neurotox Res* **2002,** 4, (7-8), 609-616.
37. Cao, J. Y.; Dixon, S. J., Mechanisms of ferroptosis. *Cell Mol Life Sci* **2016,** 73, (11-12), 2195-209.
38. Wan, J.; Ren, H.; Wang, J., Iron toxicity, lipid peroxidation and ferroptosis after intracerebral haemorrhage. *Stroke Vasc Neurol* **2019,** 4, (2), 93-95.
39. Hussain, T.; Tan, B.; Yin, Y.; Blachier, F.; Tossou, M. C.; Rahu, N., Oxidative Stress and Inflammation: What Polyphenols Can Do for Us? *Oxid Med Cell Longev* **2016,** 2016, 7432797.
40. Bai, Q.; Xue, M.; Yong, V. W., Microglia and macrophage phenotypes in intracerebral haemorrhage injury: therapeutic opportunities. *Brain* **2020,** 143, (5), 1297-1314.
41. DeGregorio-Rocasolano, N.; Marti-Sistac, O.; Gasull, T., Deciphering the Iron Side of Stroke: Neurodegeneration at the Crossroads Between Iron Dyshomeostasis, Excitotoxicity, and Ferroptosis. *Front Neurosci* **2019,** 13, 85.
42. Sousa, C.; Biber, K.; Michelucci, A., Cellular and Molecular Characterization of Microglia: A Unique Immune Cell Population. *Front Immunol* **2017,** 8, 198.
43. Dello Russo, C.; Cappoli, N.; Coletta, I.; Mezzogori, D.; Paciello, F.; Pozzoli, G.; Navarra, P.; Battaglia, A., The human microglial HMC3 cell line: where do we stand? A systematic literature review. *J Neuroinflammation* **2018,** 15, (1), 259.
44. Kierdorf, K.; Erny, D.; Goldmann, T.; Sander, V.; Schulz, C.; Perdiguero, E. G.; Wieghofer, P.; Heinrich, A.; Riemke, P.; Holscher, C.; Muller, D. N.; Luckow, B.; Brocker, T.; Debowski, K.; Fritz, G.; Opdenakker, G.; Diefenbach, A.; Biber, K.; Heikenwalder, M.; Geissmann, F.; Rosenbauer, F.; Prinz, M., Microglia emerge from erythromyeloid precursors via Pu.1- and Irf8-dependent pathways. *Nat Neurosci* **2013,** 16, (3), 273-80.
45. Salter, M. W.; Stevens, B., Microglia emerge as central players in brain disease. *Nat Med* **2017,** 23, (9), 1018-1027.
46. Tang, Y.; Le, W., Differential Roles of M1 and M2 Microglia in Neurodegenerative Diseases. *Mol Neurobiol* **2016,** 53, (2), 1181-1194.
47. Rath, M.; Muller, I.; Kropf, P.; Closs, E. I.; Munder, M., Metabolism via Arginase or Nitric Oxide Synthase: Two Competing Arginine Pathways in Macrophages. *Front Immunol* **2014,** 5, 532.
48. Mills, C. D., M1 and M2 Macrophages: Oracles of Health and Disease. *Crit Rev Immunol* **2012,** 32, (6), 463-88.

49. Orihuela, R.; McPherson, C. A.; Harry, G. J., Microglial M1/M2 polarization and metabolic states. *Br J Pharmacol* **2016,** 173, (4), 649-65.
50. Cherry, J. D.; Olschowka, J. A.; O'Banion, M. K., Neuroinflammation and M2 microglia: the good, the bad, and the inflamed. *J Neuroinflammation* **2014,** 11, 98.
51. Colonna, M.; Butovsky, O., Microglia Function in the Central Nervous System During Health and Neurodegeneration. *Annu Rev Immunol* **2017,** 35, 441-468.
52. Atri, C.; Guerfali, F. Z.; Laouini, D., Role of Human Macrophage Polarization in Inflammation during Infectious Diseases. *Int J Mol Sci* **2018,** 19, (6).
53. Picon-Pages, P.; Garcia-Buendia, J.; Munoz, F. J., Functions and dysfunctions of nitric oxide in brain. *Biochim Biophys Acta Mol Basis Dis* **2019,** 1865, (8), 1949-1967.
54. Raju, K.; Doulias, P. T.; Evans, P.; Krizman, E. N.; Jackson, J. G.; Horyn, O.; Daikhin, Y.; Nissim, I.; Yudkoff, M.; Nissim, I.; Sharp, K. A.; Robinson, M. B.; Ischiropoulos, H., Regulation of brain glutamate metabolism by nitric oxide and S-nitrosylation. *Sci Signal* **2015,** 8, (384), ra68.
55. Viola, A.; Munari, F.; Sanchez-Rodriguez, R.; Scolaro, T.; Castegna, A., The Metabolic Signature of Macrophage Responses. *Front Immunol* **2019,** 10, 1462.
56. Caldwell, R. W.; Rodriguez, P. C.; Toque, H. A.; Narayanan, S. P.; Caldwell, R. B., Arginase: A Multifaceted Enzyme Important in Health and Disease. *Physiol Rev* **2018,** 98, (2), 641-665.
57. Miao, H.; Li, R.; Han, C.; Lu, X.; Zhang, H., Minocycline promotes posthemorrhagic neurogenesis via M2 microglia polarization via upregulation of the TrkB/BDNF pathway in rats. *J Neurophysiol* **2018,** 120, (3), 1307-1317.
58. Correale, J., The role of microglial activation in disease progression. *Mult Scler* **2014,** 20, (10), 1288-95.
59. Wes, P. D.; Holtman, I. R.; Boddeke, E. W.; Moller, T.; Eggen, B. J., Next generation transcriptomics and genomics elucidate biological complexity of microglia in health and disease. *Glia* **2016,** 64, (2), 197-213.
60. Ransohoff, R. M., A polarizing question: do M1 and M2 microglia exist? *Nat Neurosci* **2016,** 19, (8), 987-91.
61. Guo, S.; Wang, H.; Yin, Y., Microglia Polarization From M1 to M2 in Neurodegenerative Diseases. *Front Aging Neurosci* **2022,** 14, 815347.
62. Wei, J.; Wang, M.; Jing, C.; Keep, R. F.; Hua, Y.; Xi, G., Multinucleated Giant Cells in Experimental Intracerebral Hemorrhage. *Transl Stroke Res* **2020,** 11, (5), 1095-1102.
63. Shtaya, A.; Bridges, L. R.; Esiri, M. M.; Lam-Wong, J.; Nicoll, J. A. R.; Boche, D.; Hainsworth, A. H., Rapid neuroinflammatory changes in human acute intracerebral hemorrhage. *Ann Clin Transl Neurol* **2019,** 6, (8), 1465-1479.
64. Bi, R.; Fang, Z.; You, M.; He, Q.; Hu, B., Microglia Phenotype and Intracerebral Hemorrhage: A Balance of Yin and Yang. *Front Cell Neurosci* **2021,** 15, 765205.
65. Zhu, H.; Wang, Z.; Yu, J.; Yang, X.; He, F.; Liu, Z.; Che, F.; Chen, X.; Ren, H.; Hong, M.; Wang, J., Role and mechanisms of cytokines in the secondary brain injury after intracerebral hemorrhage. *Prog Neurobiol* **2019,** 178, 101610.
66. Wan, S.; Cheng, Y.; Jin, H.; Guo, D.; Hua, Y.; Keep, R. F.; Xi, G., Microglia Activation and Polarization After Intracerebral Hemorrhage in Mice: the Role of Protease-Activated Receptor-1. *Transl Stroke Res* **2016,** 7, (6), 478-487.
67. Jiang, C.; Wang, Y.; Hu, Q.; Shou, J.; Zhu, L.; Tian, N.; Sun, L.; Luo, H.; Zuo, F.; Li, F.; Wang, Y.; Zhang, J.; Wang, J.; Wang, J.; Zhang, J., Immune changes in peripheral blood

and hematoma of patients with intracerebral hemorrhage. *FASEB J* **2020,** 34, (2), 2774-2791.
68. Duan, X.; Wen, Z.; Shen, H.; Shen, M.; Chen, G., Intracerebral Hemorrhage, Oxidative Stress, and Antioxidant Therapy. *Oxid Med Cell Longev* **2016,** 2016, 1203285.
69. Montaner, J.; Ramiro, L.; Simats, A.; Hernandez-Guillamon, M.; Delgado, P.; Bustamante, A.; Rosell, A., Matrix metalloproteinases and ADAMs in stroke. *Cell Mol Life Sci* **2019,** 76, (16), 3117-3140.
70. Lan, X.; Han, X.; Li, Q.; Yang, Q. W.; Wang, J., Modulators of microglial activation and polarization after intracerebral haemorrhage. *Nat Rev Neurol* **2017,** 13, (7), 420-433.
71. Li, Q.; Lan, X.; Han, X.; Durham, F.; Wan, J.; Weiland, A.; Koehler, R. C.; Wang, J., Microglia-derived interleukin-10 accelerates post-intracerebral hemorrhage hematoma clearance by regulating CD36. *Brain Behav Immun* **2021,** 94, 437-457.
72. Xi, G.; Strahle, J.; Hua, Y.; Keep, R. F., Progress in translational research on intracerebral hemorrhage: is there an end in sight? *Prog Neurobiol* **2014,** 115, 45-63.
73. Ma, Y.; Wang, J.; Wang, Y.; Yang, G. Y., The biphasic function of microglia in ischemic stroke. *Prog Neurobiol* **2017,** 157, 247-272.
74. Zhao, H.; Garton, T.; Keep, R. F.; Hua, Y.; Xi, G., Microglia/Macrophage Polarization After Experimental Intracerebral Hemorrhage. *Transl Stroke Res* **2015,** 6, (6), 407-9.
75. Thomsen, M. S.; Andersen, M. V.; Christoffersen, P. R.; Jensen, M. D.; Lichota, J.; Moos, T., Neurodegeneration with inflammation is accompanied by accumulation of iron and ferritin in microglia and neurons. *Neurobiol Dis* **2015,** 81, 108-18.
76. Urrutia, P.; Aguirre, P.; Esparza, A.; Tapia, V.; Mena, N. P.; Arredondo, M.; Gonzalez-Billault, C.; Nunez, M. T., Inflammation alters the expression of DMT1, FPN1 and hepcidin, and it causes iron accumulation in central nervous system cells. *J Neurochem* **2013,** 126, (4), 541-9.
77. McCarthy, R. C.; Sosa, J. C.; Gardeck, A. M.; Baez, A. S.; Lee, C. H.; Wessling-Resnick, M., Inflammation-induced iron transport and metabolism by brain microglia. *J Biol Chem* **2018,** 293, (20), 7853-7863.
78. Holland, R.; McIntosh, A. L.; Finucane, O. M.; Mela, V.; Rubio-Araiz, A.; Timmons, G.; McCarthy, S. A.; Gun'ko, Y. K.; Lynch, M. A., Inflammatory microglia are glycolytic and iron retentive and typify the microglia in APP/PS1 mice. *Brain Behav Immun* **2018,** 68, 183-196.
79. You, M.; Long, C.; Wan, Y.; Guo, H.; Shen, J.; Li, M.; He, Q.; Hu, B., Neuron derived fractalkine promotes microglia to absorb hematoma via CD163/HO-1 after intracerebral hemorrhage. *Cell Mol Life Sci* **2022,** 79, (5), 224.
80. Nnah, I. C.; Wessling-Resnick, M., Brain Iron Homeostasis: A Focus on Microglial Iron. *Pharmaceuticals (Basel)* **2018,** 11, (4).
81. Shay, K. P.; Moreau, R. F.; Smith, E. J.; Smith, A. R.; Hagen, T. M., Alpha-lipoic acid as a dietary supplement: molecular mechanisms and therapeutic potential. *Biochim Biophys Acta* **2009,** 1790, (10), 1149-60.
82. Rochette, L.; Ghibu, S.; Richard, C.; Zeller, M.; Cottin, Y.; Vergely, C., Direct and indirect antioxidant properties of alpha-lipoic acid and therapeutic potential. *Mol Nutr Food Res* **2013,** 57, (1), 114-25.
83. Packer, L.; Cadenas, E., Lipoic acid: energy metabolism and redox regulation of transcription and cell signaling. *J Clin Biochem Nutr* **2011,** 48, (1), 26-32.

84. Takaishi, N.; Yoshida, K.; Satsu, H.; Shimizu, M., Transepithelial transport of alpha-lipoic acid across human intestinal Caco-2 cell monolayers. *J Agric Food Chem* **2007,** 55, (13), 5253-9.
85. Khan, J.; Salhotra, S.; Ahmad, S.; Sharma, S.; Abdi, S. A. H.; Banerjee, B. D.; Parvez, S.; Gupta, S.; Raisuddin, S., The protective effect of alpha-lipoic acid against bisphenol A-induced neurobehavioral toxicity. *Neurochem Int* **2018,** 118, 166-175.
86. Yang, T.; Xu, Z.; Liu, W.; Xu, B.; Deng, Y., Protective effects of Alpha-lipoic acid on MeHg-induced oxidative damage and intracellular Ca(2+) dyshomeostasis in primary cultured neurons. *Free Radic Res* **2016,** 50, (5), 542-56.
87. Lv, C.; Maharjan, S.; Wang, Q.; Sun, Y.; Han, X.; Wang, S.; Mao, Z.; Xin, Y.; Zhang, B., alpha-Lipoic Acid Promotes Neurological Recovery After Ischemic Stroke by Activating the Nrf2/HO-1 Pathway to Attenuate Oxidative Damage. *Cell Physiol Biochem* **2017,** 43, (3), 1273-1287.
88. Ocak, H. A., E.; Bahadır, B.; Kalaycı, M.; Keskin, E.; Açıkgöz,B., Protective Effects of Alpha-Lipoic Acid on Cerebral Vasospasm in Rats. *Southern Clinics of Istanbul Eurasia* **2020,** 31, (4), 319-323.
89. Busse, E.; Zimmer, G.; Schopohl, B.; Kornhuber, B., Influence of alpha-lipoic acid on intracellular glutathione in vitro and in vivo. *Arzneimittelforschung* **1992,** 42, (6), 829-31.
90. Hultberg, B.; Andersson, A.; Isaksson, A., Lipoic acid increases glutathione production and enhances the effect of mercury in human cell lines. *Toxicology* **2002,** 175, (1-3), 103-10.
91. Choi, K. H.; Park, M. S.; Kim, H. S.; Kim, K. T.; Kim, H. S.; Kim, J. T.; Kim, B. C.; Kim, M. K.; Park, J. T.; Cho, K. H., Alpha-lipoic acid treatment is neurorestorative and promotes functional recovery after stroke in rats. *Mol Brain* **2015,** 8, 9.
92. Camiolo, G.; Tibullo, D.; Giallongo, C.; Romano, A.; Parrinello, N. L.; Musumeci, G.; Di Rosa, M.; Vicario, N.; Brundo, M. V.; Amenta, F.; Ferrante, M.; Copat, C.; Avola, R.; Li Volti, G.; Salvaggio, A.; Di Raimondo, F.; Palumbo, G. A., alpha-Lipoic Acid Reduces Iron-induced Toxicity and Oxidative Stress in a Model of Iron Overload. *Int J Mol Sci* **2019,** 20, (3).
93. Zhao, L.; Wang, C.; Song, D.; Li, Y.; Song, Y.; Su, G.; Dunaief, J. L., Systemic administration of the antioxidant/iron chelator alpha-lipoic acid protects against light-induced photoreceptor degeneration in the mouse retina. *Invest Ophthalmol Vis Sci* **2014,** 55, (9), 5979-88.
94. Koriyama, Y.; Nakayama, Y.; Matsugo, S.; Sugitani, K.; Ogai, K.; Takadera, T.; Kato, S., Anti-inflammatory effects of lipoic acid through inhibition of GSK-3beta in lipopolysaccharide-induced BV-2 microglial cells. *Neurosci Res* **2013,** 77, (1-2), 87-96.
95. Wong, A.; Dukic-Stefanovic, S.; Gasic-Milenkovic, J.; Schinzel, R.; Wiesinger, H.; Riederer, P.; Munch, G., Anti-inflammatory antioxidants attenuate the expression of inducible nitric oxide synthase mediated by advanced glycation endproducts in murine microglia. *Eur J Neurosci* **2001,** 14, (12), 1961-7.
96. Wu, M. H.; Huang, C. C.; Chio, C. C.; Tsai, K. J.; Chang, C. P.; Lin, N. K.; Lin, M. T., Inhibition of Peripheral TNF-alpha and Downregulation of Microglial Activation by Alpha-Lipoic Acid and Etanercept Protect Rat Brain Against Ischemic Stroke. *Mol Neurobiol* **2016,** 53, (7), 4961-71.

97. Tai, S.; Zheng, Q.; Zhai, S.; Cai, T.; Xu, L.; Yang, L.; Jiao, L.; Zhang, C., Alpha-Lipoic Acid Mediates Clearance of Iron Accumulation by Regulating Iron Metabolism in a Parkinson's Disease Model Induced by 6-OHDA. *Front Neurosci* **2020,** 14, 612.
98. Abobaker, A., Can iron chelation as an adjunct treatment of COVID-19 improve the clinical outcome? *Eur J Clin Pharmacol* **2020,** 76, (11), 1619-1620.
99. Carota, G.; Ronsisvalle, S.; Panarello, F.; Tibullo, D.; Nicolosi, A.; Li Volti, G., Role of Iron Chelation and Protease Inhibition of Natural Products on COVID-19 Infection. *J Clin Med* **2021,** 10, (11).
100. Camiolo, G.; Barbato, A.; Giallongo, C.; Vicario, N.; Romano, A.; Parrinello, N. L.; Parenti, R.; Sandoval, J. C.; Garcia-Moreno, D.; Lazzarino, G.; Avola, R.; Palumbo, G. A.; Mulero, V.; Li Volti, G.; Tibullo, D.; Di Raimondo, F., Iron regulates myeloma cell/macrophage interaction and drives resistance to bortezomib. *Redox Biol* **2020,** 36, 101611.
101. Kuhn, L. C., Iron regulatory proteins and their role in controlling iron metabolism. *Metallomics* **2015,** 7, (2), 232-43.
102. Liu, J. L.; Fan, Y. G.; Yang, Z. S.; Wang, Z. Y.; Guo, C., Iron and Alzheimer's Disease: From Pathogenesis to Therapeutic Implications. *Front Neurosci* **2018,** 12, 632.
103. Ma, L.; Gholam Azad, M.; Dharmasivam, M.; Richardson, V.; Quinn, R. J.; Feng, Y.; Pountney, D. L.; Tonissen, K. F.; Mellick, G. D.; Yanatori, I.; Richardson, D. R., Parkinson's disease: Alterations in iron and redox biology as a key to unlock therapeutic strategies. *Redox Biol* **2021,** 41, 101896.
104. Selim, M., Deferoxamine mesylate: a new hope for intracerebral hemorrhage: from bench to clinical trials. *Stroke* **2009,** 40, (3 Suppl), S90-1.
105. Yeatts, S. D.; Palesch, Y. Y.; Moy, C. S.; Selim, M., High dose deferoxamine in intracerebral hemorrhage (HI-DEF) trial: rationale, design, and methods. *Neurocrit Care* **2013,** 19, (2), 257-66.
106. Okauchi, M.; Hua, Y.; Keep, R. F.; Morgenstern, L. B.; Schallert, T.; Xi, G., Deferoxamine treatment for intracerebral hemorrhage in aged rats: therapeutic time window and optimal duration. *Stroke* **2010,** 41, (2), 375-82.
107. Hua, Y.; Keep, R. F.; Hoff, J. T.; Xi, G., Deferoxamine therapy for intracerebral hemorrhage. *Acta Neurochir Suppl* **2008,** 105, 3-6.
108. Zeng, L.; Tan, L.; Li, H.; Zhang, Q.; Li, Y.; Guo, J., Deferoxamine therapy for intracerebral hemorrhage: A systematic review. *PLoS One* **2018,** 13, (3), e0193615.
109. Freedman, M. H.; Boyden, M.; Taylor, M.; Skarf, B., Neurotoxicity associated with deferoxamine therapy. *Toxicology* **1988,** 49, (2-3), 283-90.
110. Levine, J. E.; Cohen, A.; MacQueen, M.; Martin, M.; Giardina, P. J., Sensorimotor neurotoxicity associated with high-dose deferoxamine treatment. *J Pediatr Hematol Oncol* **1997,** 19, (2), 139-41.
111. Fibach, E.; Rachmilewitz, E. A., Iron overload in hematological disorders. *Presse Med* **2017,** 46, (12 Pt 2), e296-e305.
112. Rostoker, G.; Vaziri, N. D., Iatrogenic iron overload and its potential consequences in patients on hemodialysis. *Presse Med* **2017,** 46, (12 Pt 2), e312-e328.
113. Kawabata, H., The mechanisms of systemic iron homeostasis and etiology, diagnosis, and treatment of hereditary hemochromatosis. *Int J Hematol* **2018,** 107, (1), 31-43.
114. Phatak, P.; Brissot, P.; Wurster, M.; Adams, P. C.; Bonkovsky, H. L.; Gross, J.; Malfertheiner, P.; McLaren, G. D.; Niederau, C.; Piperno, A.; Powell, L. W.; Russo, M. W.; Stoelzel, U.; Stremmel, W.; Griffel, L.; Lynch, N.; Zhang, Y.; Pietrangelo, A., A

phase 1/2, dose-escalation trial of deferasirox for the treatment of iron overload in HFE-related hereditary hemochromatosis. *Hepatology* **2010,** 52, (5), 1671-779.
115. Zhang, X.; Surguladze, N.; Slagle-Webb, B.; Cozzi, A.; Connor, J. R., Cellular iron status influences the functional relationship between microglia and oligodendrocytes. *Glia* **2006,** 54, (8), 795-804.
116. Kenkhuis, B.; van Eekeren, M.; Parfitt, D. A.; Ariyurek, Y.; Banerjee, P.; Priller, J.; van der Weerd, L.; van Roon-Mom, W. M. C., Iron accumulation induces oxidative stress, while depressing inflammatory polarization in human iPSC-derived microglia. *Stem Cell Reports* **2022,** 17, (6), 1351-1365.
117. Urrutia, P. J.; Borquez, D. A.; Nunez, M. T., Inflaming the Brain with Iron. *Antioxidants (Basel)* **2021,** 10, (1).
118. Gurer, H.; Ozgunes, H.; Oztezcan, S.; Ercal, N., Antioxidant role of alpha-lipoic acid in lead toxicity. *Free Radic Biol Med* **1999,** 27, (1-2), 75-81.
119. Ou, P.; Tritschler, H. J.; Wolff, S. P., Thioctic (lipoic) acid: a therapeutic metal-chelating antioxidant? *Biochem Pharmacol* **1995,** 50, (1), 123-6.
120. Biewenga, G. P.; Haenen, G. R.; Bast, A., The pharmacology of the antioxidant lipoic acid. *Gen Pharmacol* **1997,** 29, (3), 315-31.
121. Stepien, K. M.; Heaton, R.; Rankin, S.; Murphy, A.; Bentley, J.; Sexton, D.; Hargreaves, I. P., Evidence of Oxidative Stress and Secondary Mitochondrial Dysfunction in Metabolic and Non-Metabolic Disorders. *J Clin Med* **2017,** 6, (7).
122. Aquilano, K.; Baldelli, S.; Ciriolo, M. R., Glutathione: new roles in redox signaling for an old antioxidant. *Front Pharmacol* **2014,** 5, 196.
123. Maines, M. D., The heme oxygenase system: a regulator of second messenger gases. *Annu Rev Pharmacol Toxicol* **1997,** 37, 517-54.
124. Ryter, S. W.; Tyrrell, R. M., The heme synthesis and degradation pathways: role in oxidant sensitivity. Heme oxygenase has both pro- and antioxidant properties. *Free Radic Biol Med* **2000,** 28, (2), 289-309.
125. Consoli, V.; Sorrenti, V.; Grosso, S.; Vanella, L., Heme Oxygenase-1 Signaling and Redox Homeostasis in Physiopathological Conditions. *Biomolecules* **2021,** 11, (4).
126. Hoeft, K.; Bloch, D. B.; Graw, J. A.; Malhotra, R.; Ichinose, F.; Bagchi, A., Iron Loading Exaggerates the Inflammatory Response to the Toll-like Receptor 4 Ligand Lipopolysaccharide by Altering Mitochondrial Homeostasis. *Anesthesiology* **2017,** 127, (1), 121-135.
127. Tal, M. C.; Sasai, M.; Lee, H. K.; Yordy, B.; Shadel, G. S.; Iwasaki, A., Absence of autophagy results in reactive oxygen species-dependent amplification of RLR signaling. *Proc Natl Acad Sci U S A* **2009,** 106, (8), 2770-5.
128. Aguirre, A.; Lopez-Alonso, I.; Gonzalez-Lopez, A.; Amado-Rodriguez, L.; Batalla-Solis, E.; Astudillo, A.; Blazquez-Prieto, J.; Fernandez, A. F.; Galvan, J. A.; dos Santos, C. C.; Albaiceta, G. M., Defective autophagy impairs ATF3 activity and worsens lung injury during endotoxemia. *J Mol Med (Berl)* **2014,** 92, (6), 665-76.
129. Kelly, D. P.; Scarpulla, R. C., Transcriptional regulatory circuits controlling mitochondrial biogenesis and function. *Genes Dev* **2004,** 18, (4), 357-68.
130. Gleyzer, N.; Vercauteren, K.; Scarpulla, R. C., Control of mitochondrial transcription specificity factors (TFB1M and TFB2M) by nuclear respiratory factors (NRF-1 and NRF-2) and PGC-1 family coactivators. *Mol Cell Biol* **2005,** 25, (4), 1354-66.

131. Dairaghi, D. J.; Shadel, G. S.; Clayton, D. A., Human mitochondrial transcription factor A and promoter spacing integrity are required for transcription initiation. *Biochim Biophys Acta* **1995,** 1271, (1), 127-34.
132. Bhatti, J. S.; Bhatti, G. K.; Reddy, P. H., Mitochondrial dysfunction and oxidative stress in metabolic disorders - A step towards mitochondria based therapeutic strategies. *Biochim Biophys Acta Mol Basis Dis* **2017,** 1863, (5), 1066-1077.
133. Fayez, A. M.; Zakaria, S.; Moustafa, D., Alpha lipoic acid exerts antioxidant effect via Nrf2/HO-1 pathway activation and suppresses hepatic stellate cells activation induced by methotrexate in rats. *Biomed Pharmacother* **2018,** 105, 428-433.
134. Kim, S. M.; Ha, J. S.; Han, A. R.; Cho, S. W.; Yang, S. J., Effects of alpha-lipoic acid on LPS-induced neuroinflammation and NLRP3 inflammasome activation through the regulation of BV-2 microglial cells activation. *BMB Rep* **2019,** 52, (10), 613-618.
135. Hamilton, J. L.; Hatef, A.; Imran ul-Haq, M.; Nair, N.; Unniappan, S.; Kizhakkedathu, J. N., Clinically approved iron chelators influence zebrafish mortality, hatching morphology and cardiac function. *PLoS One* **2014,** 9, (10), e109880.
136. Nasrallah, G. K.; Younes, N. N.; Baji, M. H.; Shraim, A. M.; Mustafa, I., Zebrafish larvae as a model to demonstrate secondary iron overload. *Eur J Haematol* **2018,** 100, (6), 536-543.
137. Brahmachari, S.; Fung, Y. K.; Pahan, K., Induction of glial fibrillary acidic protein expression in astrocytes by nitric oxide. *J Neurosci* **2006,** 26, (18), 4930-9.
138. Nagele, R. G.; Wegiel, J.; Venkataraman, V.; Imaki, H.; Wang, K. C.; Wegiel, J., Contribution of glial cells to the development of amyloid plaques in Alzheimer's disease. *Neurobiol Aging* **2004,** 25, (5), 663-74.
139. Chen, H.; Chopp, M.; Schultz, L.; Bodzin, G.; Garcia, J. H., Sequential neuronal and astrocytic changes after transient middle cerebral artery occlusion in the rat. *J Neurol Sci* **1993,** 118, (2), 109-6.
140. Eng, L. F.; Yu, A. C.; Lee, Y. L., Astrocytic response to injury. *Prog Brain Res* **1992,** 94, 353-65.
141. Eng, L. F.; Ghirnikar, R. S., GFAP and astrogliosis. *Brain Pathol* **1994,** 4, (3), 229-37.
142. Norden, D. M.; Trojanowski, P. J.; Villanueva, E.; Navarro, E.; Godbout, J. P., Sequential activation of microglia and astrocyte cytokine expression precedes increased Iba-1 or GFAP immunoreactivity following systemic immune challenge. *Glia* **2016,** 64, (2), 300-16.
143. Memudu, A. E.; Adanike, R. P., Alpha lipoic acid reverses scopolamine-induced spatial memory loss and pyramidal cell neurodegeneration in the prefrontal cortex of Wistar rats. *IBRO Neurosci Rep* **2022,** 13, 1-8.
144. Dos Santos, S. M.; Romeiro, C. F. R.; Rodrigues, C. A.; Cerqueira, A. R. L.; Monteiro, M. C., Mitochondrial Dysfunction and Alpha-Lipoic Acid: Beneficial or Harmful in Alzheimer's Disease? *Oxid Med Cell Longev* **2019,** 2019, 8409329.
145. Molz, P.; Schroder, N., Potential Therapeutic Effects of Lipoic Acid on Memory Deficits Related to Aging and Neurodegeneration. *Front Pharmacol* **2017,** 8, 849.
146. Seifar, F.; Khalili, M.; Khaledyan, H.; Amiri Moghadam, S.; Izadi, A.; Azimi, A.; Shakouri, S. K., alpha-Lipoic acid, functional fatty acid, as a novel therapeutic alternative for central nervous system diseases: A review. *Nutr Neurosci* **2019,** 22, (5), 306-316.
147. Fiedler, S. E.; Yadav, V.; Kerns, A. R.; Tsang, C.; Markwardt, S.; Kim, E.; Spain, R.; Bourdette, D.; Salinthone, S., Lipoic Acid Stimulates cAMP Production in Healthy

Control and Secondary Progressive MS Subjects. *Mol Neurobiol* **2018,** 55, (7), 6037-6049.

148. Zhang, Y. H.; Wang, D. W.; Xu, S. F.; Zhang, S.; Fan, Y. G.; Yang, Y. Y.; Guo, S. Q.; Wang, S.; Guo, T.; Wang, Z. Y.; Guo, C., alpha-Lipoic acid improves abnormal behavior by mitigation of oxidative stress, inflammation, ferroptosis, and tauopathy in P301S Tau transgenic mice. *Redox Biol* **2018,** 14, 535-548.